# Geographic information system-based spatio-temporal detection and mapping of COVID–19 hot/cold spots in Oman

**Yaseen Al–Mulla[1,2], Mohammed Al–Muqaimi[1], Ahsan Ali[1], Taif Al–Badi[1], Krishna Parimi[1], Anusha Chowdary[1]**
[1]Remote Sensing and GIS Research Center, Sultan Qaboos University, Al–Khod, Muscat, Oman
[2]Department of Soils, Water and Agricultural Engineering, Sultan Qaboos University, Al–Khod, Muscat, Oman

**Article Info**

***Article history:***

Received Dec 16, 2023
Revised Jul 3, 2024
Accepted Jul 17, 2024

***Keywords:***

Cold spots
COVID–19
Geographic information system
Hot spots
Inverse distance weighted analysis

**ABSTRACT**

Infected COVID-19 patients, especially after March 11, 2020, grew drastically in Oman. Hence, a variety of measures were issued to restrict all social gatherings, commercial activities, and mandating preventative health practices. This study aimed to i) understand distribution patterns and impact of decisions and responses at the spread of confirmed cases; ii) highlight and verify most concentrated regions with infections; and iii) overview spatial changes of cases overtime. The analysis was carried out using inverse–distance-weighted interpolation and hotspot (Getis–Ord GI*) techniques. Results showed a substantial relationship between spatial structure of COVID–19 and population distribution and density. COVID–19 has increased by 11.5% weekly in the capital, which were locked down since April 2020. However, after health quarantine was lifted on May 29, 2020, weekly cases surged in the capital. Al-Batinah-North and Dhofar recorded an increase of 32.1% and 30.5%, respectively, after restrictions had eased. The analysis illustrated that spread of COVID–19 was shifting from Northeast to Southeast and later shifted back to the Northeast of the country at the end of year 2022. This study is beneficial for pertinent organizations to perform detailed studies for developing and monitoring disease systems and dominating relevant factors.



***Corresponding Author:***

Yaseen Al–Mulla
Remote Sensing and GIS Research Center, Sultan Qaboos University
Al–Khod, Muscat 123, Oman
Email: yalmula@squ.edu.om

## 1. INTRODUCTION

On December 31, 2019, the Wuhan Municipal Health Commission announced an outbreak of viral pneumonia of unknown causes in Wuhan, People's Republic of China. On January 8, 2020, the Chinese Center for Disease Control and Prevention officially stated that the causative pathogen of viral pneumonia was a novel coronavirus [1]. The World Health Organization (WHO) then followed the virus's emergence in collaboration with the People's Republic of China's Health Committee, and the WHO stated in February that the sickness caused by the novel coronavirus disease of 2019 to be known as COVID–19 [2].

COVID–19 spread concerned the global public health sector, producing over 118,319 infected and 4,292 deaths in over 100 countries by March 11, 2020 [3]. As a result, the WHO concluded COVID–19 was a pandemic. Since that time, the number of affected cases has increased and spread globally. In less than a month, there were ten times as many COVID–19 cases in April 2020 as there were in March [4]. All countries continue to track infected cases daily and take several actions to identify ways to stop the spread of illness within their communities by adhering to all precautionary guidelines and instructions set by the WHO.

Over 163 million individuals worldwide have contracted COVID–19, which has also caused over 3.9 million fatalities [5]. The outbreak of COVID–19 also affected the sultanate of Oman like other countries in the world. The Ministry of Health in Oman reported the first registration of two coronavirus cases that were related to traveling to a southwestern Asian country [6], [7]. Since February 24, 2020, the number of cases was recorded low (< 5 cases) for several weeks. On March 10, 2020, the supreme committee (SC) for COVID–19 was established by His Majesty Sultan Haitham Bin Tariq ordering various decisions to prevent the outbreak of COVID–19 in the country [8]. The number of infected patients grew drastically in the Sultanate of Oman provinces (Governorates). Daily data of confirmed cases revealed the spread of the pandemic in specific places caused by communal transmission of the virus. As a result, the SC issued a variety of measures to restrict all social gatherings and commercial activity on a national level. Additionally, they mandated preventative health practices including wearing a facemask, refraining from shaking hands, and maintaining social distance.

In March 2020, the SC decided to impose a set of restrictions (for two and a half months) which also included a lockdown and limiting 30 percent of total workers in workplaces as reported cases surged in Oman [9]. On May 31, 2020, the authorities relaxed the lockdown by allowing 50% of all public employees to return to their work and subsequently opening the markets, while imposing strict restrictions and guidelines to be followed. However, the number that was documented increased dramatically in one and a half months to 62,574, with 40,090 instances of recovery, 22,194 cases of sickness, and 290 cases of death [10]. Based on this the government re-ordered the decrease of public office workers back to 30%. Figure 1 illustrates how confirmed, sick, and death cases progressed since the start of the pandemic in Oman in February and until mid–July 2020.

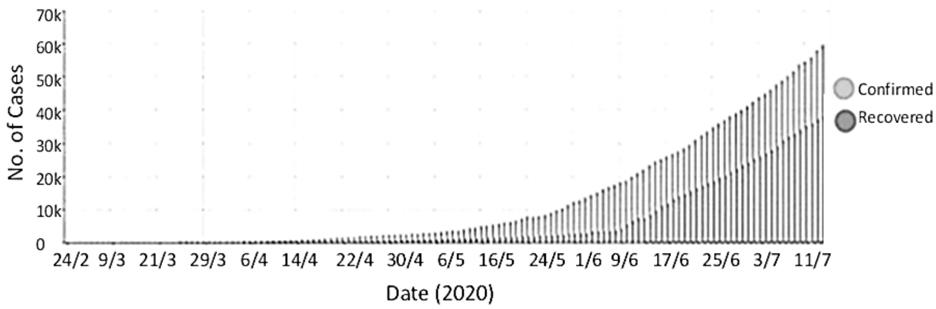


Figure 1. Progress of confirmed sick and death cases since the start of the pandemic in Oman until mid–July 2020

The transmission of coronavirus can incidence by direct contact with infected people or with surfaces in the immediate environment or with objects used by the infected people [11]. The average time from exposure to COVID–19 to symptoms onset was 5 to 6 days and in many cases ranged from 1 to 14 days [12]. Therefore, the spatial element and time are the most important factors that determine the spread pattern of infections. Geographic information system (GIS) provides high capabilities and methods to find where the infected people are, as well as to figure out if there are spatial patterns of the outbreak of COVID–19. GIS has been used in many health studies [13] particularly in monitoring Malaria [14], [15], plant population [16], dengue and chikungunya [17], and COVID–19 [18]. GIS can also map the changes of the outbreak over time, examine the factors that affect the distribution of the disease, and give indications about the disease trend and hotspots [19]. Given the population in the Sultanate of Oman, does not exceed 4,472,000 people [20] these numbers of confirmed, sick and deaths give an urgent need to utilize the advanced tools to help in analyzing the pandemic situation in the country. This information can guide the deployment of healthcare personnel, testing facilities, and vaccination campaigns to the area's most in need. By focusing efforts on hot spot areas, authorities can effectively curb the transmission of the virus and prevent its further spread into surrounding regions.

The use of GIS for the hot spot analysis of COVID–19 has become essential worldwide for understanding and monitoring the disease development [21]–[25]. GIS facilitates the investigation and analysis of geographical data, enabling health authorities and policymakers to pinpoint COVID–19 "hot spots", or regions with increased COVID–19 cases. GIS makes it easy to identify trends, clusters, and patterns in viral propagation, allowing for swift and precise treatments. Al Kindi *et al.* [26] observed the spatial and temporal patterns of COVID–19 spread and provided the preliminary basis to investigate the impacts of restrictions and guidelines on the COVID–19 spread in the total period of only 8–weeks. Another studies [27], [28] examined the relationship between COVID–19 and social, physical, and economic factors in Oman using empirical spatial modelling techniques. They reported a correlation between the migrant's proportion and their workplaces and found the significance of GIS-based hot spot analysis for effective communication of COVID–19 data to the public. Visualizing the spatial distribution of cases through maps and interactive dashboards helps individuals understand the localized impact of the virus and encourages them to adopt preventive measures. It also enables the dissemination of accurate and up–to–date information about testing locations, vaccination centers, and containment measures, empowering individuals to make informed decisions and take appropriate actions. Hence, the hot spot analysis of COVID–19 using GIS is crucial for understanding the spatial dynamics of the disease, targeting interventions, identifying risk factors, and communicating with the public. By harnessing the power of GIS, health authorities and policymakers can effectively respond to the pandemic, mitigate its impact, and protect public health. On the local scale, A few studies have used the GIS platform to analyze the pattern of COVID–19 outbreaks spatially and temporally. Our study stands unique in its application of hot spot/cold spot and spatio–temporal analysis using GIS based on overall spatial and temporal tracking of the COVID–19 cases for more than 95 weeks. To our knowledge, this is the first study in Oman discussing the impact of guidelines taken to limit the outbreak of the COVID–19 crisis by using hot spot/cold spot analysis and spatio–temporal tools. One of the major strengths of this study is the spatial-temporal coverage of the data used in this study in addition to the impact assessment of the directives issued by the SC. Moreover, very limited studies reported ways of propagation of COVID–19 to set policies and guidelines to limit the movement of the coronavirus. Hence, this study aimed i) to investigate the implementation of geo-temporal/spatial analysis in order to understand the distribution patterns and the impact of decisions and responses at the spread of confirmed cases; ii) to highlight and verify the most concentrated regions with infections in Oman; and iii) to overview the spatial changes of cases overtime pre, during, and after the lockdown. This study can help in leading more research to develop and detect possible hotspots in highly populated areas, help understand the spatial dynamics of COVID–19 spread, guiding public health initiatives including expanding access to healthcare services, putting community outreach programs into place, or addressing socioeconomic disparities that might be a factor in the concentration of cases in certain regions.

## 2. METHOD

### 2.1. Study area

The Sultanate of Oman is located in the southeast of the Arabian Peninsula, along the Arabian Sea, and shares a border with Saudi Arabia, United Arab Emirates, and Yemen. The total area of Oman is 309,500 square kilometers [29]. The population in 2020 was 4.471 million people giving the country a population density of 15 people per square kilometer [30]. The Sultanate of Oman includes eleven governorates in Figure 2 named Ad Dakhiliyah, Ad Dhahirah, Al Batinah North, Al Batinah South, Al Buraimi, Al Wusta, Ash Sharqiyah North, Ash Sharqiyah South, Dhofar, Musandam, and Muscat (capital of the country). Each governorate is divided into *wilayats* (provinces) [29]. Many lockdowns and specific guidelines were issued periodically in particular governorates to control the increase in COVID–19 cases.

### 2.2. Data collection

In this study, data on the cumulative incidence of COVID–19 cases registered at the Ministry of Health, Oman from May 2020 to February 2022 was used as a main source for data used in this study. Locations of registered COVID–19 cases were collected from the “Tarassud Plus” mobile application, which was powered by the Ministry of Health, Oman. On the other hand, population data across the *Wilayats* of Oman was collected from the National Center for Statistical Information [20]. The official account of the efforts of countering COVID–19 is used as a reference to find out the timeline of decisions during the pandemic [9].

### 2.3. Modelling approach

The main platform used for the analysis is GIS technology by which geo–statistical analysis of inverse distance weighted (IDW) interpolation was conducted of all positive COVID–19 cases for all *wilayats* in the Governorates of Oman. Many studies have shown the effectiveness of using the selected modeling approach in infectious disease transmission and spread [19], [28], [31]–[38] [39]–[44]. The IDW interpolation works on the basis that the similarity of nearby monitored cases is more than those that are farther from each other [19]. This mechanism assists in the prediction algorithm for all places that lack records of monitored cases and so the farther the distance of the monitored cases from prediction places the less weight in comparison to those that are close to the prediction places as illustrated in Figure 3 [45].

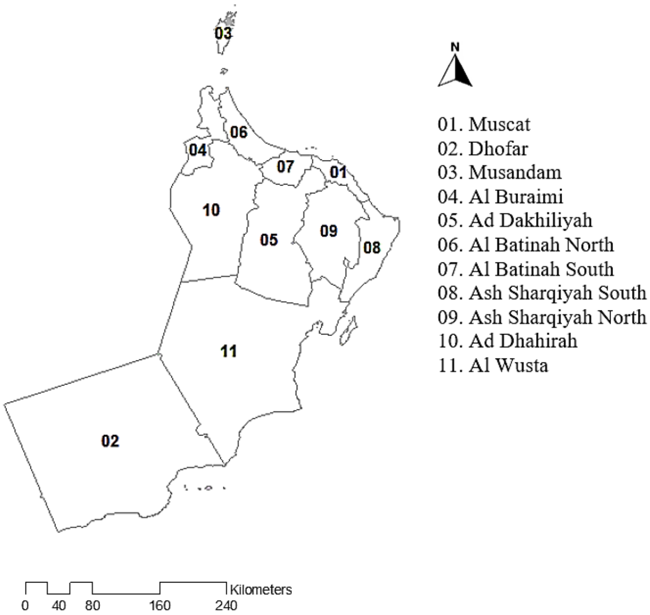


Figure 1. Names and locations of Governorates of the Sultanate of Oman [20]

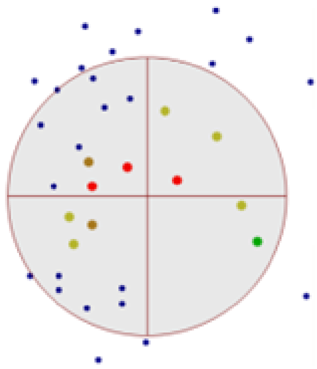

Figure 2. Weights assigned to each monitored data point

The analysis involved the temporal percentage of infections according to government guidelines. The analysis also incorporated the identification of hotspots in the governorates. Ancillary data from the lockdown in the governorate was used to study the effect of the lockdown on the infection rate.

### 2.4. Spatial distribution of COVID–19 pattern across the *Wilayats* of Oman

Inverse distance weighted (IDW) is a type of deterministic method for multivariate interpolation with a known scattered set of points. It is used to predict the values for any undetermined destination by calculating the predicted zone of the adjacent areas [46]. Based on two inferences: first, the impact of the unknown value of a point was specifically extended to the point of close control rather than to the point of the range. Second, the extent of the impact was related to the inverse of the range between the points. The equation (1) was used for the analysis [47], [48].

$$\mathrm{Zp} = \frac{\sum_{i=1}^{n}\left(\frac{z_i}{d_i^p}\right)}{\sum_{i=1}^{n}\left(\frac{1}{d_i^p}\right)} \tag{1}$$

Where $Z_i$ is the value of the known points, $Zp$ refers to the unknown point, controls the significance of the control point $Z_i$ and *n* is the nearest vicinity of the control points which is usually required to consume time.

$d_i^p$ refers to the interpolated point, $p$ is a weighting absolute value that is an arbitrary positive real number, and $p$ is equal to 1 in inverse distance weighting [49].

### 2.5. Hotspot analysis of COVID–19 pattern across the Governorates of Oman

Hotspot analysis (Getis–Ord GI*) is considered a helpful tool to recognize spatial clusters of both high and low values and has previously been applied to model several disease outbreaks [23]. This tool functions by examining each characteristic concerning its surrounding features. Although a high-value feature is intriguing, it could not be a statistically significant hot spot. To be a statistically significant hot spot, a feature must have a high value and be surrounded by other features with high values as well. In addition, to be interested in locating areas with unexpectedly high values in relation to some other variable, which is the population in this study [50].

GIS hotspot technology identifies statistically significant spatial clusters of high–confirmed COVID–19 cases as “hot spots” and low numbers of cases as “cold spots”. The results are exported in an output feature class with a z–score, p-value, and confidence level bin (*Gi_Bin*) for each feature in the input feature class. *Gi_Bin* values are used to detect statistically significant hot and cold regions, which are then corrected for multiple testing and spatial dependency using the false discovery rate (FDR) correction technique.

$$G_i^* = \frac{\sum_{j=1}^{n} w_{i,j}x_j - \overline{X}\sum_{j=1}^{n} w_{i,j}}{S\sqrt{\frac{\left[n\sum_{j=1}^{n} w_{i,j}^2 - \left(\sum_{j=1}^{n} w_{i,j}\right)^2\right]}{n-1}}} \quad (2)$$

where $x_j$ is the attribute value for feature $j$, $w_{i,j}$ is the spatial weight between feature $i$ and $j$, $n$ is equal to the total number of features, and:

$$\overline{X} = \frac{\sum_{j=1}^{n} x_j}{n} \quad (3)$$

$$S = \sqrt{\frac{\sum_{j=1}^{n} x_j^2}{n} - (\overline{x})^2} \quad (4)$$

while $G_i^*$ statistic is a z–score.

### 2.6. Spatial autocorrelation (Moran’s index)

Prior to the implementation of the Hotspot analysis, Moran’s index was used to statistically analyze the feature pattern of the dataset to determine if that was clustered, scattered, or random. The Moran’s index statistic for spatial autocorrelation was calculated as directed by study [51] as shown (5).

$$I = \frac{n}{S_0}\frac{\sum_{i=1}^{n}\sum_{j=1}^{n} w_{i,j} z_i z_j}{\sum_{j=1}^{n} z_j^2} \quad (5)$$

where $Z_i$ is the deviation of an attribute for $i$ from its mean ($x$i $-\overline{x}$ ), $w_{i,j}$ is the spatial weight between feature $i$ and $j$, $n$ is equal to the total number of features, and $S_0$ is the aggregate of all the spatial weight:

$$S_0 = \sum_{i=1}^{n}\sum_{j=1}^{n} w_{i,j} \quad (6)$$

The $Z_I$– score for the statistic is computed as (7):

$$Z_I = \frac{I - E[I]}{\sqrt{V\,[I]}} \quad (7)$$

where:

$$E[I] = -\frac{1}{n-1} \quad (8)$$

and

$$V\,[I] = E[I^2] - E\,[I]^2 \quad (9)$$

## 3. RESULTS AND DISCUSSION

### 3.1. Spread and change in the number of confirmed cases of COVID–19

The progression of the total cases during the pandemic was examined in the study on three levels: pre-lockdown, during the lockdown, and after the lockdown. According to the [20], Mutrah has the third–highest population (230,881) in Oman with the highest density of 2565.3 people per $Km^2$, following Bawshar (population of 382,184), and As Seeb (population of 478,517). Among all *wilayat* of the Governorate of Muscat, COVID–19 concentrated initially in the *Wilayat* of Mutrah. Later, the weekly cases in Mutrah reduced week by week throughout the lockdown, from 1556 cases on May 6, 2020, to 87 cases in August 2020, with a dramatic decreasing tendency. However, after May 18, 2020, when the SC decided to permit several commercial and industrial sectors to resume activities, and after lifting the lockdown on May 29, 2020, infection in other *Wilayats* of Muscat Governorate increased, reaching the highest confirmed cases in As Seeb and Bawshar. The remaining *wilayat* in this governorate have a population of less than 130,000 people in each of them as presented in Table 1.

Table 1. Population and density of the Muscat Governorate

| No. | *Wilayat* name | Population (2020) | Density |
|---|---|---|---|
| | | No. of People | People per $Km^2$ |
| 1 | As Seeb | 478517 | 979 |
| 2 | Bawshar | 382184 | 1124.1 |
| 3 | Mutrah | 230881 | 2565.3 |
| 4 | Al Amerat | 121103 | 113.4 |
| 5 | Qurayyat | 58438 | 38.1 |
| 6 | Muscat | 31317 | 114.3 |

Results of IDW interpolation for Muscat Governorate in Figure 4 shows the spread of the disease originated from Mutrah to the *Wilayats*. Figure 4 shows the number of confirmed cases and the COVID–19 spread across *Wilayats* of Muscat Governorate. Figure 4(a) shows the number of cumulative cases since the beginning of the pandemic up to May 6, 2020. Where the rate of increase in confirmed cases is concentrated primarily in Mutrah compared to other *Wilayats* in Muscat. A moderate spread observed in As Seeb and Bawshar, which ranges from 100 to 500 cases. The lowest range (1 to 100) was observed in Al Amerat, Muscat and Qurayyat.

In an effort to stop the COVID–19 from spreading throughout the country, the SC implemented control points between governorates on Wednesday, April 1, 2020, shuttered Muscat Governorate, and quarantined the Mutrah *Wilayat*. In addition, employees were exempt from attending the workplace. On May 4, it was decided to isolate the Wadi Al Kabir industrial area in Mutrah *Wilayat* from the rest of the *wilayat* to monitor and control the rise in cases.

Figure 4(b) depicts a decline in confirmed cases from 5.1% to 4.8% in the governorate that is most likely attributed to isolated Mutrah and Wadi Al Kabir, but the pandemic's expansion steadily grew in the *Wilayats* of Bawshar and As Seeb. Figures 4(a) and 4(b) show a modest rise in the number of confirmed cases during the Governorate of Muscat's isolation, with Mutrah as a prominent *wilayat*. As indicated in Figure 4(c), the number of confirmed cases increased in the *Wilayat* of As Seeb, which recorded 60.9% (1,102) increase. However, the number of confirmed cases increased between May 18 and May 29 to 3,035 cases. The decision to allow a set of commercial and industrial operations to restart after May 18, 2020, might be one of the major reasons for the surge in cases.

To facilitate movement between all Governorates of Oman and the continuation of economic operations, the SC decided to lift the isolation of Muscat Governorate from other governorates with effect from May 29, 2020. Moreover, the maximum limit of the workers in the public offices was increased from 30% to 50%. Figures 4(d) to 4(g) demonstrate the highest rates (51%) as the lockdown in Muscat Governorate was lifted and limitations were loosened. The government published offenders' names and images in different media on July 7, which may have contributed to the relative decline in the number of cases as indicated in Figure 4(h). Moreover, due to an increase in cases, the SC decided on July 25 to impose a movement ban and close all businesses from 7:00 p.m. to 6:00 a.m. until August 8; this decision was later extended until August 15.

During the above period, less confirmed cases were reported in Figures 4(i) and 4(j). Figure 4(i) illustrates that the confirmed cases dropped (during the first 10 days) with a rate of -182% (1,782) as compared with pre–lockdown (5,037). As–Seeb reported the highest confirmed cases (652) as compared to other *Wilayats*. Figure 4(j) depicts the number of confirmed cases from 10 to 20 days after the ban and limitations were imposed. All the *Wilayats* in the Governorate of Muscat had a significant drop in the number of confirmed cases during this time. Table 2 represents confirmed cases and decision timelines in all *Wilayats* of Muscat. Figure 5 shows the cumulative and confirmed cases of COVID–19 cases in the Muscat Governate.

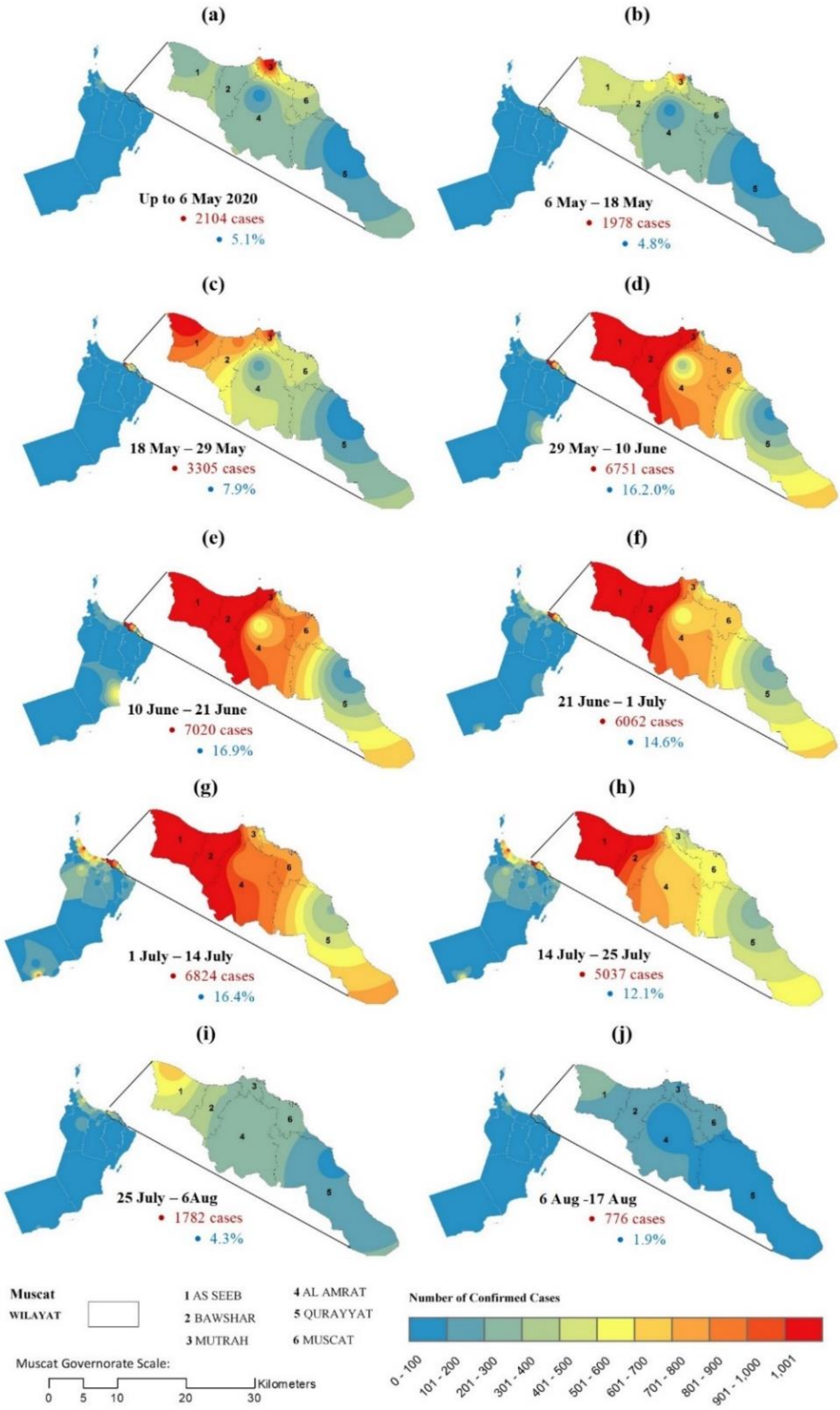


Figure 4. IDW interpolation of Muscat Governorate with varying timeline: (a) since the beginning of the pandemic up to May 6, 2020, (b) between May 6 to May 18, 2020, (c) between May 18 to May 29, 2020, (d) between May 29 to June 10, 2020, (e) between June 10 to June 21, 2020, (f) between June 21 to July 1, 2020, (g) between July 1 to July 14, 2020, (h) between July 14 to July 25, 2020, (i) between July 25 to August 6, 2020, and (j) between August 6 to August 17, 2020

Table 2. The confirmed cases and decisions for Muscat *Wilayats* within the timeline from May to August 2020

| Date<br>*Wilayat* | Until<br>6 May | 6–18<br>May | 18–29<br>May | 29 May –<br>10 Jun | 10–21<br>Jun | 21 Jun –<br>1 July | 1–14<br>Jul | 14 – 25<br>Jul | 25 July –<br>6 Aug | 6–17<br>Aug |
|---|---|---|---|---|---|---|---|---|---|---|
| As Seeb | 260 | 430 | 1,102 | 2,625 | 2,794 | 2,478 | 2,831 | 2,283 | 652 | 260 |
| Bawshar | 215 | 516 | 826 | 2,110 | 2,079 | 1,766 | 1,609 | 1,081 | 301 | 138 |
| Mutrah | 1,556 | 954 | 1,163 | 1,404 | 1,297 | 909 | 788 | 421 | 258 | 87 |
| Al Amerat | 54 | 60 | 159 | 342 | 498 | 509 | 810 | 623 | 242 | 59 |
| Qurayyat | 3 | 4 | 16 | 84 | 93 | 181 | 294 | 260 | 83 | 47 |
| Muscat | 16 | 14 | 39 | 186 | 259 | 219 | 492 | 369 | 246 | 185 |
| Decisions | *A | | *B | | *C | | | | *D | |

A 1. Isolate Muscat Governorates
2. Prevent employees from attending workplaces.
3. Isolate Mutrah and Wadi Al Kabir.
4. Nationwide lockdown during Ramadan (20 April–24 May)

B 1. Allowing a package of commercial and industrial activities.

C 1. Lifting the health closure on the Governorate of Muscat (with the continued isolation of the *Wilayat* of Mutrah and Wadi Al Kabir Industrial Area).
2. Allowing new package of commercial and industrial activities.

D 1. Banning movement and shutting down all public places and shops from 7:00 p.m. to 6:00 a.m. until August 8th, when the decision was extended until August 15th.

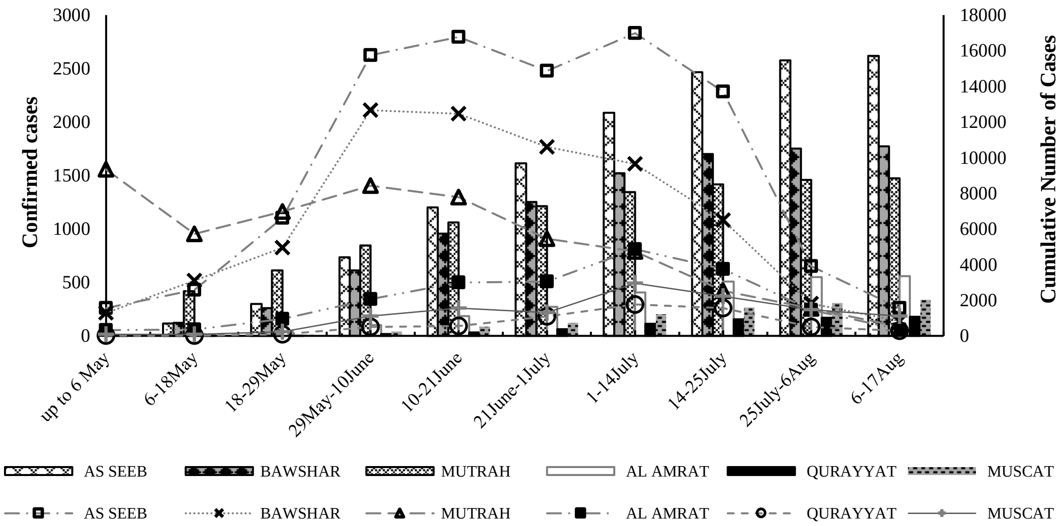


Figure 5. Cumulative (bars) and daily confirmed cases (curved lines) of Muscat Governorate May-August 2020)

Figure 6 shows the IDW interpolation of Al Wusta Governorate. Figures 6(a) to 6(i) illustrates the fluctuation in the number of confirmed cases before, during, and after the lockdown. Figure 6(a) shows that the spread of pandemic throughout the Al Wusta was below 100 cases from the start of the pandemic until May 29, 2020. According to Figure 6(b), there was a sharp increase in the number of cases reported in the first two weeks of June in the *Wilayat* of Ad Duqm, going from 0.5% of confirmed cases by May 29, 2020, to 33.95% by June 12, 2020. The highest number of cases (587) were recorded prior to the SC's decision on June 13, 2020 to quarantine Ad Duqm to stop the pandemic from spreading to other *Wilayat* in Al Wusta.

Figure 6(c) illustrates the decline in confirmed cases in Ad Duqm over the two weeks of quarantine, from 33.9% to 28%. The quarantine period had been extended twice until August 15, 2020. The number of infections throughout the quarantine period in Figures 6(c)-(f) decreased from 66 cases to 17 cases. The number of confirmed cases in Ad Duqm began to decline from the second week of June and eventually reached 1% by August 17, 2020. This impact of quarantine on the number of confirmed cases coincides with the results from a study by Meo *et al.* [52] that reported an identical statement on the impact of the quarantine on the declined new cases of COVID–19 during the quarantine period. A rise in confirmed cases was recorded in the *Wilayat* of Al Jazir, according to Figure 6(d), reaching a moderate level of more than 100 cases. From July 25, 2020, the SC decided to lock down all marketplaces and public places from 7:00 p.m. to 6:00 a.m., until August 15, 2020. While the decision to lock down and isolate Ad Duqm came to an end on August 15, 2020.

After the lockdown was lifted, the percentage of confirmed cases rose to 17.5%, as shown in Figure 6(g). However, the SC imposed a movement ban in all the governorates from 8:00 p.m. to 5:00 a.m. starting from October 11 to October 24, 2020. Based on these decisions, the percentage of confirmed cases decreased to 4.3% by November 8, 2020, and all *Wilayat* of Al Wusta recorded the minimum number of cases as shown in Figure 6(h). Two weeks later, the cases increased again to 7.3% in Figure 6(i) and the range of cases reported was between 100 and 500.

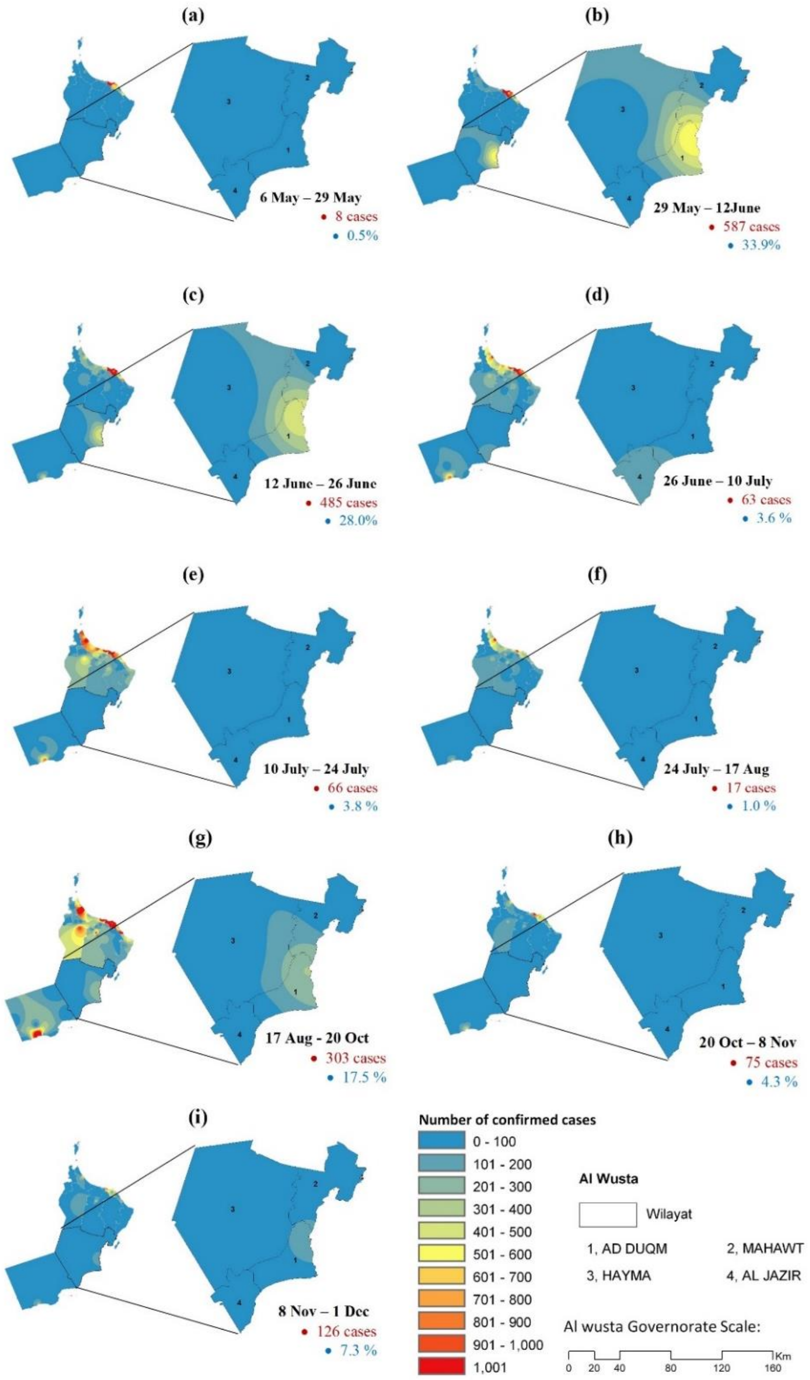


Figure 6. IDW interpolation of Al Wusta Governorate with varying timeline: (a) between May 6 to May 29, 2020, (b) between May 29 to June 12, 2020, (c) between June 12 to June 26, 2020, (d) between June 26 to July 10, 2020, (e) between July 10 to July 24, 2020, (f) between July 24 to August 17, 2020, (g) between August 17 to October 20, 2020, (h) between October 20 to November 8, 2020, and (i) between November 8 to December 1, 2020

Population and density data in Table 3 was recorded from May 2020 to December 2020 for interpolation and the timeline of decisions. According to Table 4, the *Wilayat* of Ad Duqm, which has the biggest population, had the highest rate of rise in confirmed cases. Figure 7 shows the cumulative and confirmed cases of COVID–19 cases in the Al Wusta Governorate.

Table 3. Population and density of the Al Wusta Governorate

| No. | *Wilayat* name | Population (2020) | Density |
|---|---|---|---|
| | | No. of People | People per Km$^2$ |
| 1 | Ad Duqm | 19,221 | 2.05 |
| 2 | Muhut | 17,385 | 1.34 |
| 3 | Hayma | 10,093 | 0.18 |
| 4 | Al Jazer | 5,645 | 0.81 |

Table 4. The confirmed cases and decisions for Al Wusta *Wilayats* within the timeline from May to December 2020

| Date *Wilayat* | Up to 29 May | 29 May – 12 Jun | 12 Jun – 26 Jun | 26 Jun – 10 Jul | 10 – 24 Jul | 24 Jul – 17 Aug | 17 Aug – 20 Oct | 20 Oct – 8 Nov | 8 Nov – 1 Dec |
|---|---|---|---|---|---|---|---|---|---|
| HAYMAA | 7 | 30 | 12 | 68 | 26 | 18 | 47 | 5 | 5 |
| AD DUQM | 8 | 587 | 485 | 63 | 66 | 17 | 303 | 75 | 126 |
| AL JAZIR | 0 | 0 | 27 | 120 | 34 | 17 | 21 | 3 | 3 |
| MAHAWT | 0 | 0 | 0 | 8 | 13 | 2 | 7 | 4 | 1 |
| Decisions | A | | | 13 June – 15 August | | | | | |
| | B | | | | | 25 Jul – 15 Aug | | | |
| | C | | | | | | 11 – 24 October | | |

A*: Isolate *Wilayat* of Ad Duqm.
B*: Banning movement and shutdown of all public places and shops from 7:00 pm to 6:00 am until 8th August when the decision was extended up to 15 August.
C*: Banning movement and shutdown all public places and shops from 8:00 pm to 5:00 am.

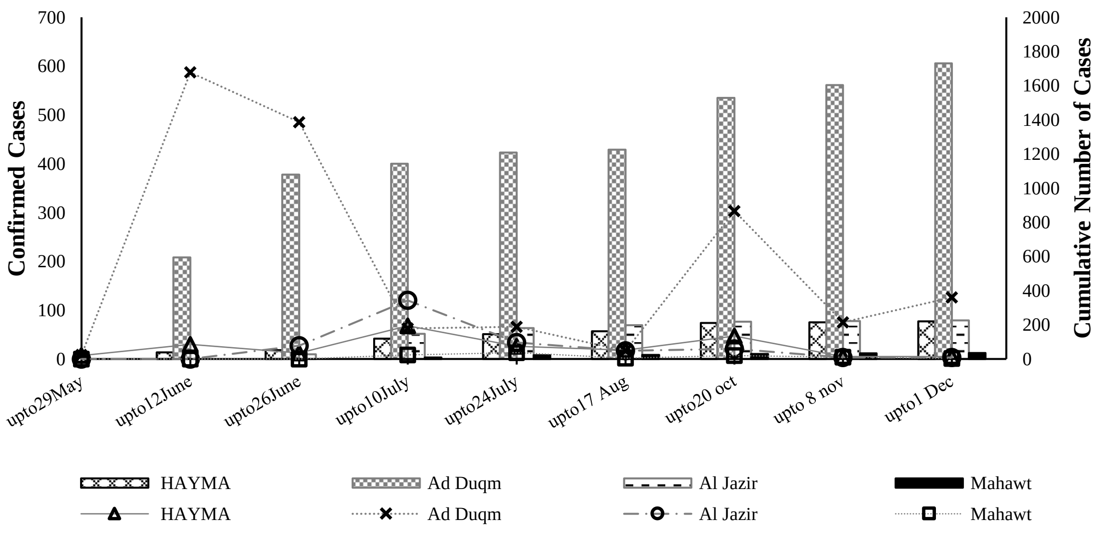


Figure 7. Cumulative (bars) and daily confirmed cases (curved lines) of Al Wusta Governorate (May – December 2020)

Figure 8 shows the temporal changes using IDW interpolation for the Al Batinah North Governorate, from May 2020 to January 2021. Coinciding with the beginning of the pandemic, the government prevented employees from coming to workplaces and decided to close shops and businesses. However, the COVID-19 spread was consistently escalating. Figures 8(a) to 8(c) present the spread of COVID–19 before the lockdown. Results from Figures 8(a) and 8(b) revealed that the rate of confirmed cases with COVID–19 rose from 1.0% to 6.5%, respectively. The SC relaxed its decision to close the markets on

May 18, 2020, by allowing some commercial sectors to gradually restart operations. Additionally, the decision to ban employees from going to work was relaxed on May 31, 2020, enabling 50% of employees in firms to go to workplaces.

Figure 8(c) represents the rapid rise (32.1%) in COVID–19 cases from June 15, 2020, to July 15, 2020. Based on that, the government declared a countrywide ban on July 25, 2020. The enforced ban included market closures and a mobility ban for two weeks beginning on August 8, 2020, which was then extended until August 15. Figure 8(d) shows the results during the lockdown, when the percentage of confirmed cases fell to 27.7%. Figures 8(e) to 8(h) shows the confirmed cases in every *wilayat* have decreased from 22.3% to 1.1% because of the SC decision throughout the country to ban movement, commercial activities and activation of polymerase chain reaction (PCR) tests on arrivals to country during the August 15, 2020, January 3, 2021. As shown in Table 5 the most populated *Wilayats* in the Al Batinah North Governorate are Sohar, As Suwayq, and Saham, where the rate of rise in confirmed cases was mostly focused. Table 6 provides data for interpolation during the study period. Figure 9 shows the cumulative and confirmed cases of COVID–19 in the Al Batinah North Governorate.

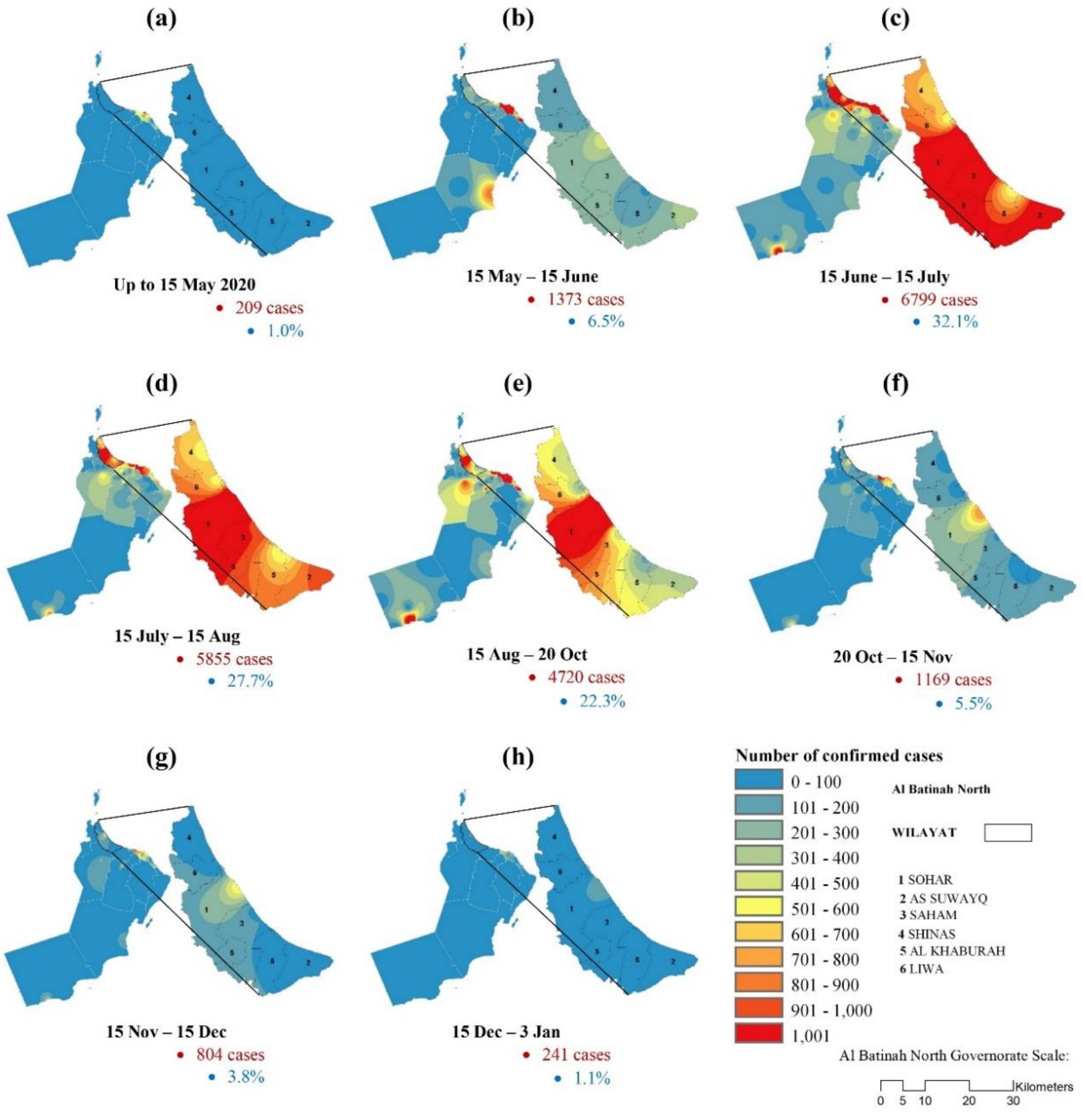


Figure 8. IDW interpolation of Al Batinah North Governorate with varying timeline: (a) since the beginning of the pandemic up to May 15, 2020, (b) between May 15 to June 15, 2020, (c) between June 15 to July 15, 2020, (d) between July 15 to August 15, 2020, (e) between August 15 to October 20, 2020, (f) between October 20 to November 15, 2020, (g) between November 15 to December 15, 2020, (h) between December 15, 2020 to January 3, 2021

Table 5. Population and density of the Al Batinah North Governorate

| No. | *Wilayat* name | Population (2020) | Density |
|---|---|---|---|
| | | No. of People | People per $Km^2$ |
| 1 | As Suwayq | 184,561 | 183.2 |
| 2 | Liwa | 55,698 | 75.2 |
| 3 | Shinas | 82,741 | 77.3 |
| 4 | Saham | 150,057 | 100.4 |
| 5 | Al Khaburah | 78,775 | 50.5 |
| 6 | Sohar | 232,849 | 115 |

Table 6. The confirmed cases and decision for Al Batinah North from May to January 2021

| Date | | Until | 15 May – | 15 Jun – | 15 Jul – | 15 Aug – | 20 Oct – | 15 Nov – | 15 Dec 20 – |
|---|---|---|---|---|---|---|---|---|---|
| *Wilayat* | | 15 May | 15 Jun | 15 Jul | 15 Aug | 20 Oct | 15 Nov | 15 Dec | 3 Jan 21 |
| As Suwayq | | 48 | 343 | 1549 | 958 | 366 | 110 | 73 | 27 |
| Liwa | | 12 | 143 | 554 | 536 | 279 | 52 | 32 | 13 |
| Shinas | | 44 | 123 | 596 | 544 | 395 | 82 | 44 | 7 |
| Saham | | 26 | 217 | 1217 | 947 | 408 | 87 | 79 | 22 |
| Al Khaburah | | 17 | 89 | 534 | 496 | 181 | 53 | 21 | 3 |
| Sohar | | 62 | 458 | 2349 | 2374 | 3091 | 785 | 555 | 169 |
| Decision | A | Until 31 May | | | | | | | |
| | B | | 18 May – 25 July | | | | | | |
| | C | | | | | | From 7 July | | |
| | D | | | | 25 Jul – 15 Aug | | | | |
| | E | | | | | 1 Oct – 1 Nov | | | |
| | F | | 11–24 Oct | | | 11–24 Oct | | | |
| | G | | | | | | | From 1 Nov | |

A: Prevent employees from attending workplaces. Allowing a package of commercial and industrial activities (28 April).
B: Allowing packages of commercial and industrial to resume their activities gradually. (18 May) (10 June) (23 June). The decision preventing employees from attending workplaces ended by allowing 50% of employees to attend the workplaces. (31 May)
C: Increasing the penalties for violators of the decisions by publishing the names and pictures of the violators in the various media. (7July)
D: Banning movement and shutdown all public places and shops from 7:00 pm to 6:00 am until 8th August when the decision was extended until 15 August.
E: Allowing those who hold a valid residence permit to return to the Sultanate, must provide that they undergo a Polymerase Chain Reaction test (PCR) upon return and be quarantined for 14 days.
F: Banning movement and shutdown all public places and shops from 8:00 pm to 5:00 am.
G: Providing a PCR test and not exceeding 96 hours to enter the country and quarantined for 8 days. Preventing entry to and exit from the Sultanate through various ports (22 Dec).

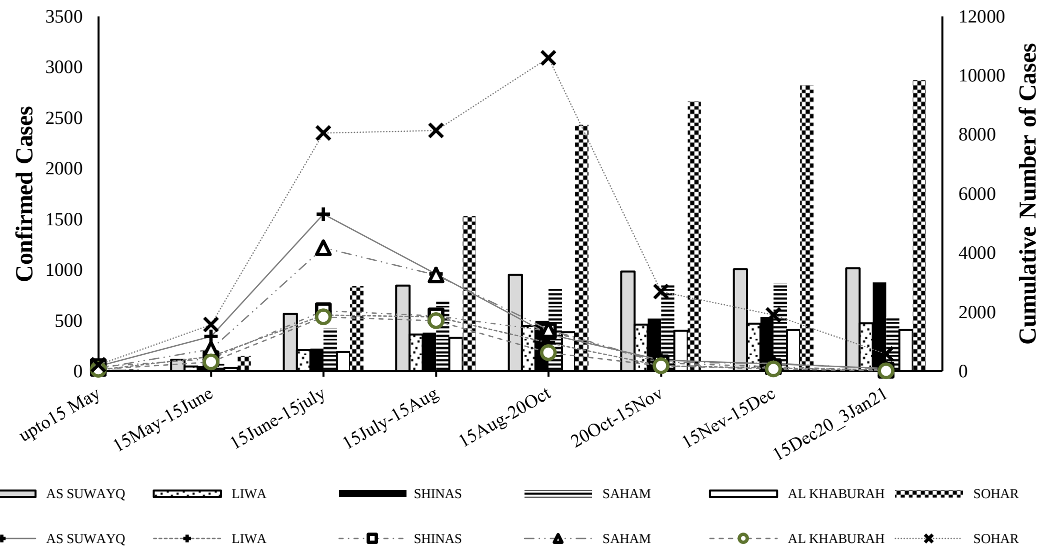


Figure 9. Cumulative (bars) and daily confirmed cases (curved lines) of Al Batinah North Governorate (May 2020 – January 2021)

In the Dhofar Governorate, the tourism season runs from May until early September. Due to the COVID–19, SC decided to close Dhofar governorate on June 13 to October 1, 2020, to limit the spread of the COVID–19. Salalah, the governorate's most populous *wilayat*, has the highest rate of increasing confirmed cases. With a total population of 331949 in 2020 as shown in Table 7, Salalah had a population density of 67 persons per $Km^2$, which was 79% of Dhofar's total population.

Table 7. Population and density of the Dhofar Governorate

| No. | *Wilayat* name | Population (2020) | Density |
|---|---|---|---|
| | | No. of People | People per $km^2$ |
| 1 | Salalah | 331,949 | 67.14 |
| 2 | Taqah | 21,487 | 20.47 |
| 4 | Mirbat | 16,364 | 19.04 |
| 4 | Thumrayt | 17,113 | 0.46 |
| 5 | Al Mazyunah | 8,399 | 0.59 |
| 6 | Shalim wa Juzr Alhalanyat | 6,339 | 0.33 |
| 7 | Rakhyut | 4,985 | 2.99 |
| 8 | Dalkut | 3,179 | 4.56 |
| 9 | Maqshin | 627 | 0.03 |
| 10 | Sadah | 6,016 | 1.92 |

Spatial maps were constructed from the data of COVID–19 distributions across the *Wilayats* of Dhofar in Figure 10. Figures 10(a) and 10(b) exhibits the spatial distribution of COVID–19 prior to the government's decision to isolate Dhofar Governorate on June 13, 2020. The spread began in Salalah in Figure 10(b) with the moderate range above 100 to 500 cases after the SC agreed from 18 May to gradually restart a package of commercial and industrial operations, while other *Wilayats* were in the minimum range of infection from zero to 100 cases. In the first month of isolation, from 15 June to 15 July, the weekly cases increased by 30.5% in the *wilayat* of the Dhofar Governorate as shown in Figure 10(c). Salalah reported 1,655 cases at the end of the isolation period which was the highest number of confirmed cases in the governorate, at that time. On the other side, Mirbat also had moderate infections with 100–500 cases, whereas the lowest number of cases were reported in other *Wilayats*.

The SC decided that all public places and businesses must be closed at night from 7:00 p.m. to 6:00 a.m. from July 25 to August 8, 2020. It was further decided to prolong this decision until August 15, 2020. Figure 10(d) shows a 47% decline in confirmed cases during the Dhofar Governorate's isolation and the night movements ban. During this time, Salalah witnessed a drop in cases from its peak of moderate levels (between 500–900), while the remaining *Wilayats* continued to register fewer than 100 COVID–19 cases.

Figure 10(e) shows the distribution of the spatial distribution of COVID–19 after the decision of lifting the isolation in Dhofar Governorate. As a result, between August 15 to October 20, 2020, the COVID–19 spread rapidly, with the *Wilayat* of Salalah witnessing the largest concentration of infections. During the research period, the Dhofar Governorate recorded the highest number of COVID–19 cases, accounting for 39.1 % of the total number of cases.

The number of confirmed cases decreased from 39.1% to 8.6% and later 4.9% in Figures 10(f) and 10(g). The main cause for the reduction is most likely due to the SC's decision to re–close all stores and public venues from October 11 to 24, 2020, after all beaches were banned until March 20, 2021. Furthermore, all travelers arriving in the Sultanate from November 1, 2020, through all ports with a PCR test report no more than 96 hours before arrival, as well as another test upon arrival. Table 8 shows the recorded data from May 2020 to December 2020 for the spatial analysis while the timeline of cumulative and confirmed cases of Dhofar Governorate during the study period as shown in Figure 11.

The trend of COVID–19 distribution in the Ash Sharqiyah North Governorate from February 2021 to July 2021 is depicted in Figure 12. Al Mudaybi is the governorate's largest *wilayat* in terms of area covered, accounting for 42% of the governorate's population. Ibra and Bidiyah make up 18.4% and 15.6% of the governorate's total population, respectively. Ibra has the highest density in the governorate with 41 residents per $Km^2$. The increase in confirmed cases in the *Wilayat* of Al Mudaybi can be seen in Figures 12(a) and 12(b) since the COVID–19 monitoring was initiated. On February 12, 2021, the SC decided to close all public sites and parks in the governorates. Furthermore, all commercial operations in Ash Sharqiyah North were prohibited from 7:00 p.m. to 6:00 a.m. for two weeks.

The government prolonged the closure order to March 20, 2021. Furthermore, the SC decided to reduce the number of employees in workplaces by 70% from March 21 to April 4. Nonetheless, the number of confirmed cases increased from 3.6 % to 18.4% in this period as shown in Figures 12(a) to 12(c). Al Mudaybi and Ibra had the largest number of infected cases (100–500), whereas other *wilayats* recorded the lowest number of infections. As a result, on March 28, the SC decided to limit the movement of individuals and vehicles entering or leaving the Governate. Furthermore, commercial operations were prohibited at night from 8 p.m. to 5 a.m. in all Governorates of the Sultanate of Oman until April 8, 2020, when the night closure decision extended, although persons and cars were permitted to travel until April 13, 2021. Figure 12(d) represents the spatial assessment of COVID–19 in the holy month of Ramadan when the SC decided to impose many decisions to limit the spread of the COVID–19 including movement bans and limited commercial activity. This might lead decrease in COVID–19 cases in Al–Mudaybi from 530 to 343 cases, and in Ibra from 230 to 186 cases by the end of Ramadan.

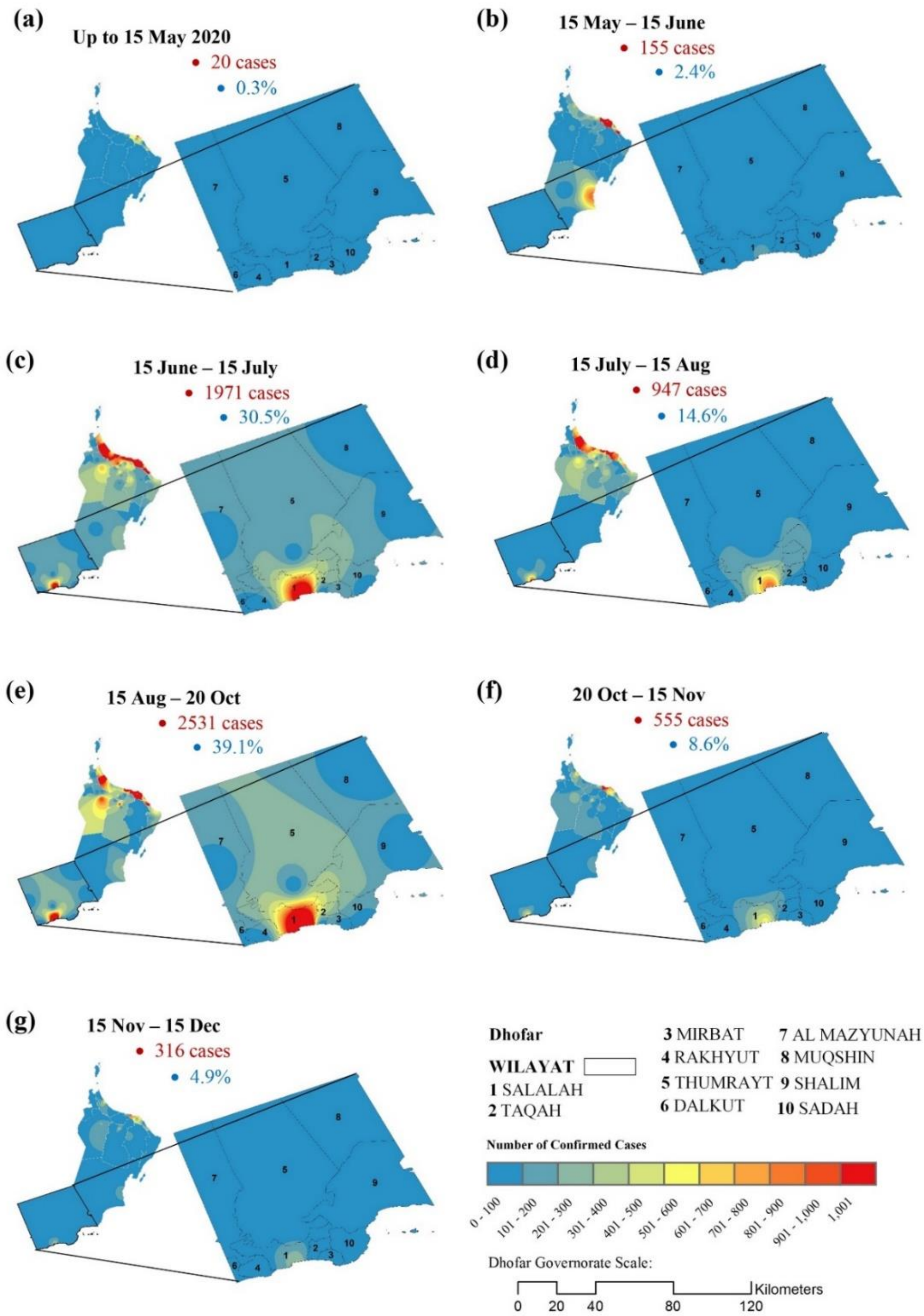


Figure 10. IDW interpolation of Dhofar Governorate with varying timeline: (a) since the beginning of the pandemic up to May 15, 2020, (b) between May 15 to June 15, 2020, (c) between June 15 to July 15, 2020, (d) between July 15 to August 15, 2020, (e) between August 15 to October 20, 2020, (f) between October 20 to November 15, 2020, (g) between November 15 to December 15, 2020, (h) between December 15, 2020 to January 3, 2020

Table 8. The confirmed cases of Dhofar *Wilayats* within the timeline from May to November 2020

| Date / *Wilayat* | Until 15 May | 15 May – 15 Jun | 15 Jun – 15 Jul | 15 Jul – 15 Aug | 15 Aug – 20 Oct | 20 Oct – 15 Nov |
|---|---|---|---|---|---|---|
| Salalah | 20 | 138 | 1655 | 875 | 2409 | 529 |
| Al Mazyunah | 0 | 2 | 44 | 11 | 15 | 0 |
| Shalim wa Juzr Alhalanyat | 0 | 14 | 36 | 20 | 30 | 1 |
| Mirbat | 0 | 1 | 167 | 0 | 7 | 3 |
| Taqah | 0 | 0 | 14 | 6 | 26 | 3 |
| Thumrayt | 0 | 0 | 46 | 15 | 31 | 16 |
| Rakhyut | 0 | 0 | 5 | 5 | 2 | 3 |
| Dalkut | 0 | 0 | 4 | 8 | 4 | 0 |
| Maqshin | 0 | 0 | 0 | 1 | 0 | 0 |
| Sadah | 0 | 0 | 0 | 1 | 7 | 0 |
| Decision A | Until 31 May | | | | | |
| Decision B | | 18 May – 25 July | | | | |
| Decision C | | | 13 June – 1 October | | | |
| Decision D | | | From 7 July | | | |
| Decision E | | | | 25 Jul – 15Aug | | |
| Decision F | | | | | 1 Oct – 1 Nov | |
| Decision G | | | | | 11 – 24 Oct | |
| Decision H | | | | | | 1 Nov |

A. Prevent employees from attending workplaces.
B. Allowing commercial and industrial to resume their activities gradually, (May 18) (June 10) (June 23). Preventing employees from attending workplaces ended by allowing 50% of employees to attend (31 May).
C. Closing the Governorate of Dhofar and banning entry to the governorate.
D. Increasing the penalties for violators by publishing the names and pictures in the various media (July 7).
E. Banning movement and shutdown all public places and shops from 7:00 pm to 6:00 am until 8th August when the decision was extended until 15 August.
F. Allowing those who hold a valid residence permit to return to the Sultanate, must provide that they undergo a PCR test upon return and quarantined for 14 days.
G. Banning movement and shutdown all public places and shops from 8:00 pm to 5:00 am.
H. Providing a PCR test and not exceeding 96 hours to enter the Country and quarantined for 8 days.

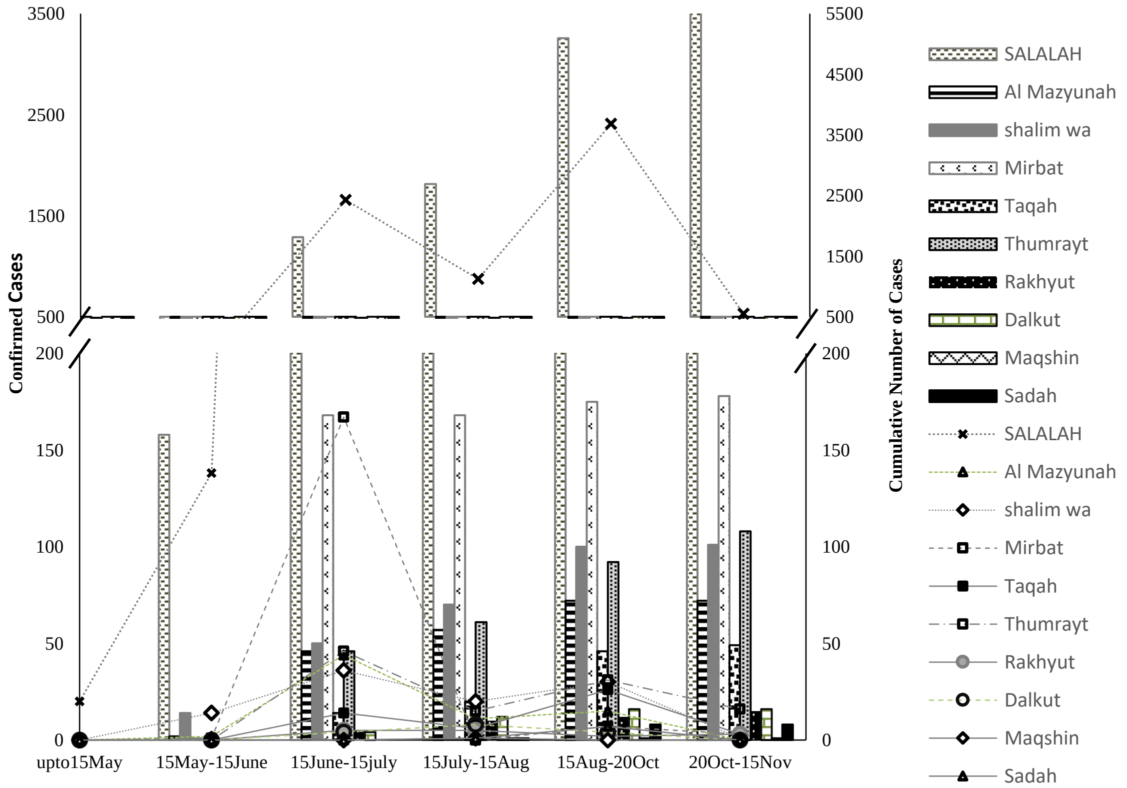


Figure 11. Cumulative (bars) and daily confirmed cases (curved lines) of Dhofar Governorate (May – November 2020)

Figure 12(e) shows that confirmed cases continued to fall in North Sharqiyah Governorate in the first two weeks after the decisions, with the percentage of confirmed cases reaching 7.4% (total cases 364). On June 5, 2021, the government eased a set of restrictions; and decided to allow reopening of mosques with a capacity of not less than one hundred worshipers, reopening exhibitions, wedding halls and other collective commercial activities with a limit of 30% of the capacity and allowing gyms to not exceeded 50% of their capacity. That allowance might lead to the results in Figure 12(f). Spatial analysis showed that the increase in infections reached 16.6% of cases (820 cases) and this percentage raised to 18.1% by the end of June 2021 in Figure 12(g). As a result, the government decided on 20 June 2021 returning to reclose all shops and public places and prohibit all movements between 8:00 p.m. and 4:00 a.m. Figure 12(h) represented the result during 3 weeks of the restrictions where the number of cases decreased gradually to 13.6% and later 3% and in the subsequent period from July 15 to July 25 in Figure 12(i). Table 9 refers to the population data in the governorate and Table 10 refers to the confirmed cases that were used for the interpolation and the decision timeline. Figure 13 shows the cumulative number of infections and the fluctuation in confirmed cases from February 2021 to July 2021.

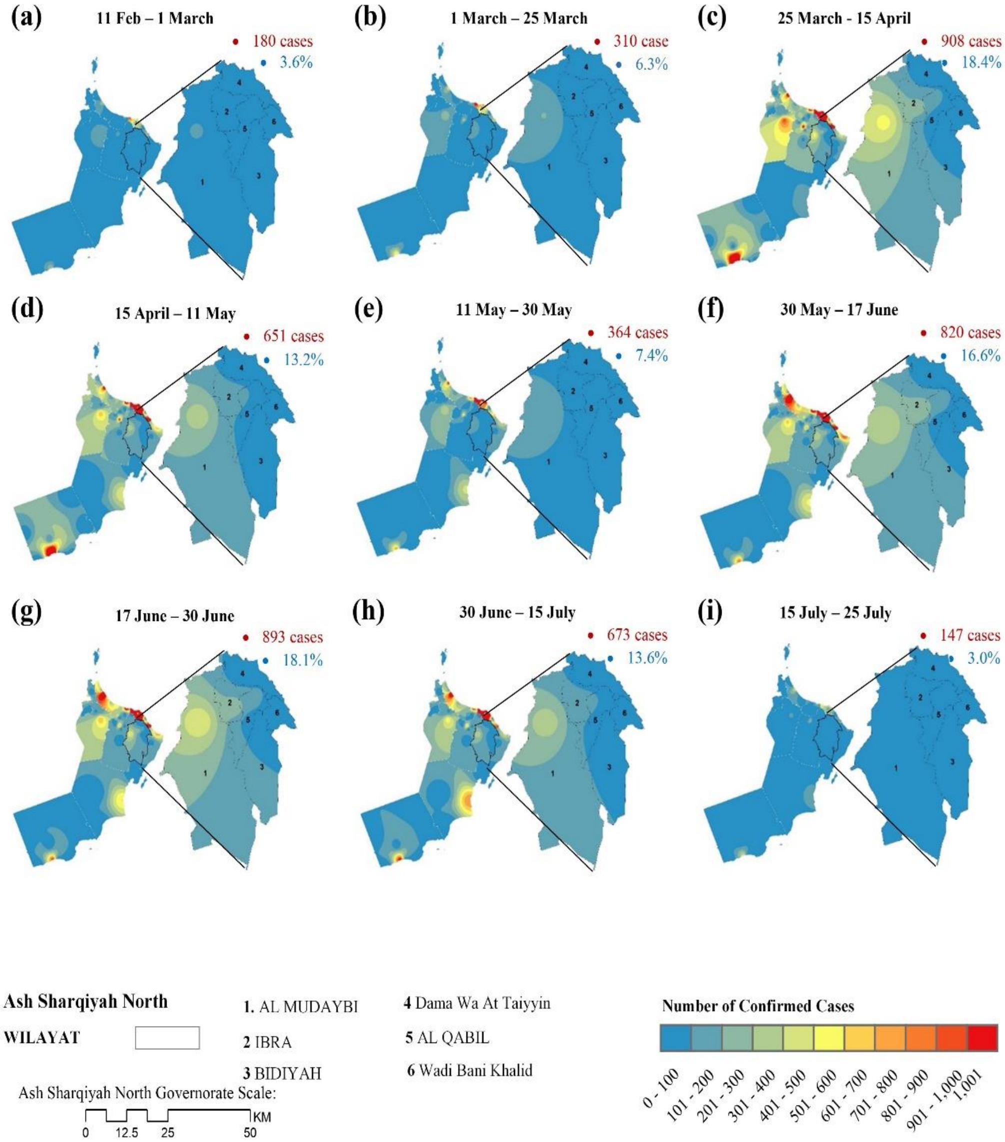


Figure 12. IDW interpolation of As Sharqiyah North Governorate with varying timeline: (a) between February 11 to March 1, 2020, (b) between March 1 to March 25, 2020, (c) between March 25 to April 15, 2020, (d) between April 15 to May 11, 2020, (e) between May 11 to May 30, 2020, (f) between May 30 to June 17, 2020, (g) between June 17 to June 30, 2020, (h) between June 30 to July 15, 2020, and (i) between July 15 to July 25, 2020

Table 9. Population and density of the Ash Sharqiyah North Governorate

| No. | *Wilayat* name | Population (2020) No. of People | Density People per $Km^2$ |
|---|---|---|---|
| 1 | Al Mudaybi | 114806 | 9 |
| 2 | Ibra | 50189 | 41 |
| 3 | Bidiyah | 42530 | 12 |
| 4 | Al Qabil | 24824 | 15 |
| 5 | Wadi Bin Khalid | 12980 | 15 |
| 6 | Dama Wa At Taiyyin | 26493 | 16 |

Table 10. The confirmed cases and decision of Ash Sharqiyah North within the timeline from February to July 2021

| Date *Wilayat* | 11 Feb – 1 Mar | 1 Mar – 25 Mar | 25 Mar – 15 Apr | 15 Apr – 11 May | 11 May – 30 May | 30 May – 17 Jun | 17 Jun – 30 Jun | 30 Jun – 15 Jul | 15 Jul – 25 Jul |
|---|---|---|---|---|---|---|---|---|---|
| Al Mudaybi | 106 | 202 | 530 | 343 | 175 | 376 | 476 | 354 | 78 |
| Al Qabil | 11 | 6 | 21 | 17 | 17 | 45 | 46 | 26 | 9 |
| Bidiyah | 13 | 22 | 81 | 75 | 67 | 93 | 88 | 71 | 17 |
| Ibra | 40 | 64 | 230 | 186 | 95 | 271 | 242 | 184 | 35 |
| Dama Wa At Taiyyin | 8 | 12 | 33 | 23 | 7 | 24 | 28 | 17 | 6 |
| Wadi Bani Khalid | 2 | 4 | 13 | 7 | 3 | 11 | 13 | 21 | 2 |
| Decision A | 12 Feb – 20 Mar | | | | | | | | |
| Decision B | | | 21 Mar – 4 Apr | | | | | | |
| Decision C | | | | 18 Mar – 13 May | | | | | |
| Decision D | | | | | 8 – 15 May | | | | |
| Decision E | | | | | | 5 – 20 Jun | | | |
| Decision F | | | | | | | | 20 Jun – 31 Jul | |

A. Closure of all commercial activities in the Ash Sharqiyah North Governorate (7:00 pm – 6:00 am).
B. Reducing the number of employees in workplaces to 70% of the total number of employees.
C. Night closure of commercial activities and prevention of movement of people and vehicles.
D. Block all business activities throughout the day.
E. A set of easing the restriction decisions:
(Allowing groups to do sports activities, allowing using beaches and public parks, reopening of exhibitions, wedding halls and other collective commercial activities, allowing gyms to open (50%) of their capacity, allowing Omanis and GCC residents to travel across land border to their workplaces, reopening mosques whose capacity in not less than 100 prayers.
F. Banning movement and shutdown all public places and shops from 8:00 pm to 4:00 am

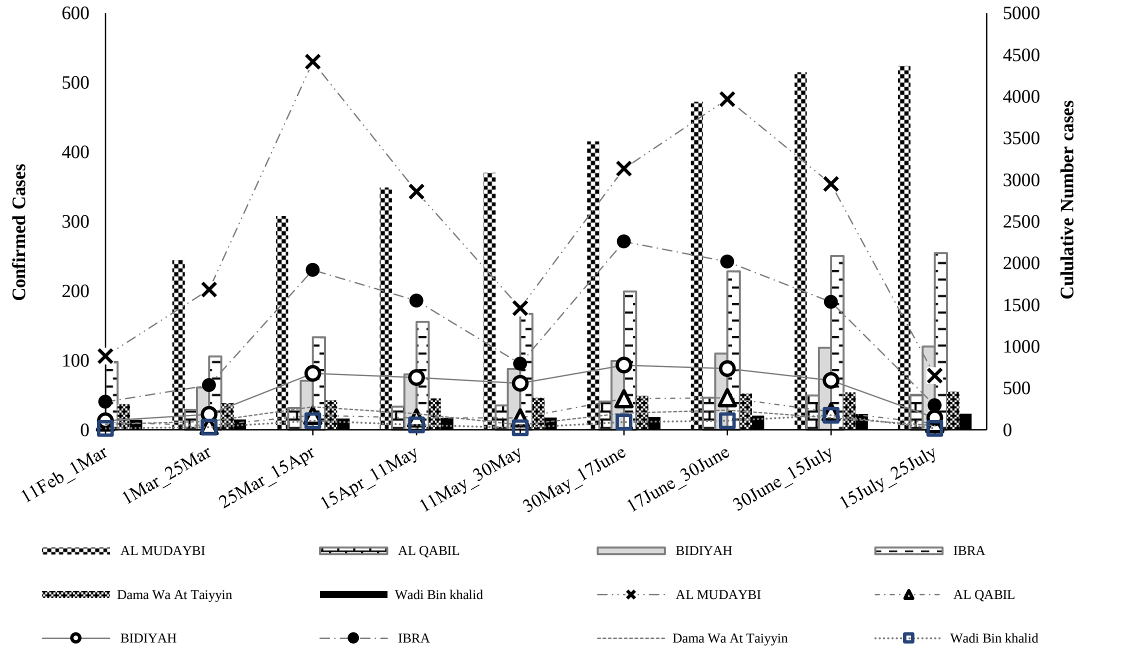


Figure 13. Cumulative (bars) and daily confirmed cases (curved lines) of Ash Sharqiyah North Governorate (Feb – July 2021)

### 3.2. Hotspot analysis

As shown in Figure 14, the z–score for this research was positive (5.49), and there was less than a 1% probability that this clustered pattern could have formed by chance. The positive Moran's index value suggests a propensity toward clustering when the z–score or p–value indicates statistical significance, whereas a negative Moran's index value indicates a tendency toward dispersion. To produce statistically significant clustering, which supports the underlying spatial precondition used in the hot spot analysis, the null hypothesis must be rejected. The null hypothesis in this situation asserts that the features' values are spatially uncorrelated. Hence, this result indicates a substantial relationship between the spatial structure of the COVID–19 epidemic and the population distribution and density.

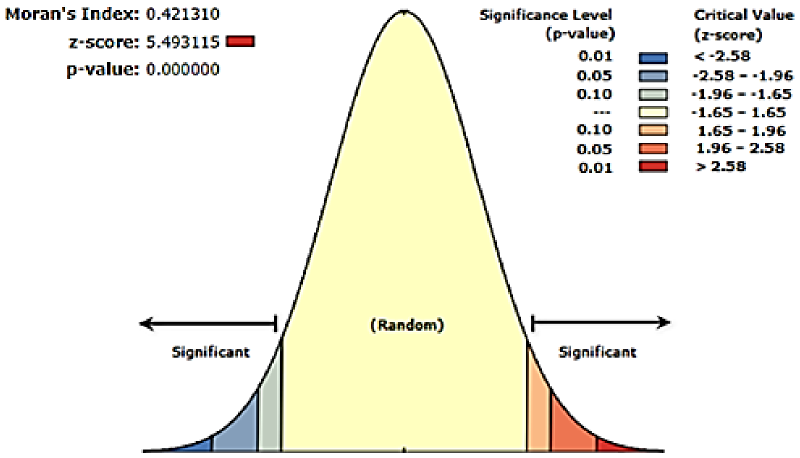


Figure 14. Moran's index result

The hotspots spatial intensity estimated for the COVID–19 confirmed cases is shown in Figure 15 and the spatial distribution of confirmed cases shows high variability in the hotspot clusters. Figure 15(a) represents the start weeks of the pandemic, where Muscat Governorate was the only hotspot across the country with highest confidence rate in the *Wilayats* of Mutrah, Muscat and Al Amerat, whereas Bawshar recorded lower intensity of infections with 90% of intensity scale. While all other *Wilayats* classified as not significant according to the confirmed cases.

Figure 15(b) represents that by third week of July, the cold spot in Ad Duqm converted to a hotspot region with high confidence rate of 99%, whereas the intensity of infections in Mutrah, Muscat and Al Amerat dropped off to 95% comparing to *Wilayat* of Ad Duqm. From October 11, 2020, until October 24, 2020, the SC decided to ban movement, shut down all public places and shops from 8:00 p.m. until 5:00 a.m., shut down all beaches until further notice, reclose some activities, and publish the names and photos of the violators in the media. As of November 1, 2020, the SC mandated that all visitors entering the Sultanate through all ports must submit to a PCR test no later than 96 hours before their arrival and another test after they have arrived. The SC agreed on December 22, 2020, to prohibit passenger travel from crossing air, land, and sea borders for a week, except for freight aircraft, ships, and trucks. The government asked to use the electronic wristband at all crossings on December 29, 2020, to monitor the traveler's movement in quarantine period.

These applied restrictions controlled the intensity in Ad Duqm to decrease from high rate in Figure 15(b) to 95% in Figure 15(c), "Not significant" in Figure 15(d). Meanwhile the intensity of infections in the *Wilayat* of Bawshar, Muscat, Mutrah and Al Amerat increased. Figures 15(d)–(f) show that Muscat, Mutrah, Al Amerat and Bawshar are the only *wilayat* classified as a hotspot among all the country. Figure 15(g) shows a rise in the hotspots areas over the year of 2022 where As Seeb reached the high rate of intensity and *Wilayat* of Bidbid added to the hotspots areas. Other *Wilayats* across the country maintained as "Not significant" over the period of pandemic of COVID–19.

This study provided spatial maps of COVID–19 spread across the sultanate of Oman, the results of this study especially in the Muscat Governate coincide with the results from a similar study conducted by [26] that used data for only 8 weeks of data in the year 2020. The situation in the Mutrah, AS Seeb and Bowsher was worse as compared with the other *Wilayats* of other Governate in year 2020 but this study used 95 weeks of consecutive data for the COVID–19 spread and found that the hot spot was located in Muscat but with less confidence value. The hot spot analysis illustrates the spread of COVID–19 was shifting from North East to South East and later shifted back to Northeast at the end of year 2022; this same trend was observed in [26] for the year 2020 only. The advantages of such two–dimensional hotspot surface representations, particularly of pandemic analysis provided a more realistic continuous model for identification of hotspot patterns with respective to COVID–19 infection rate across the country, over space and time.

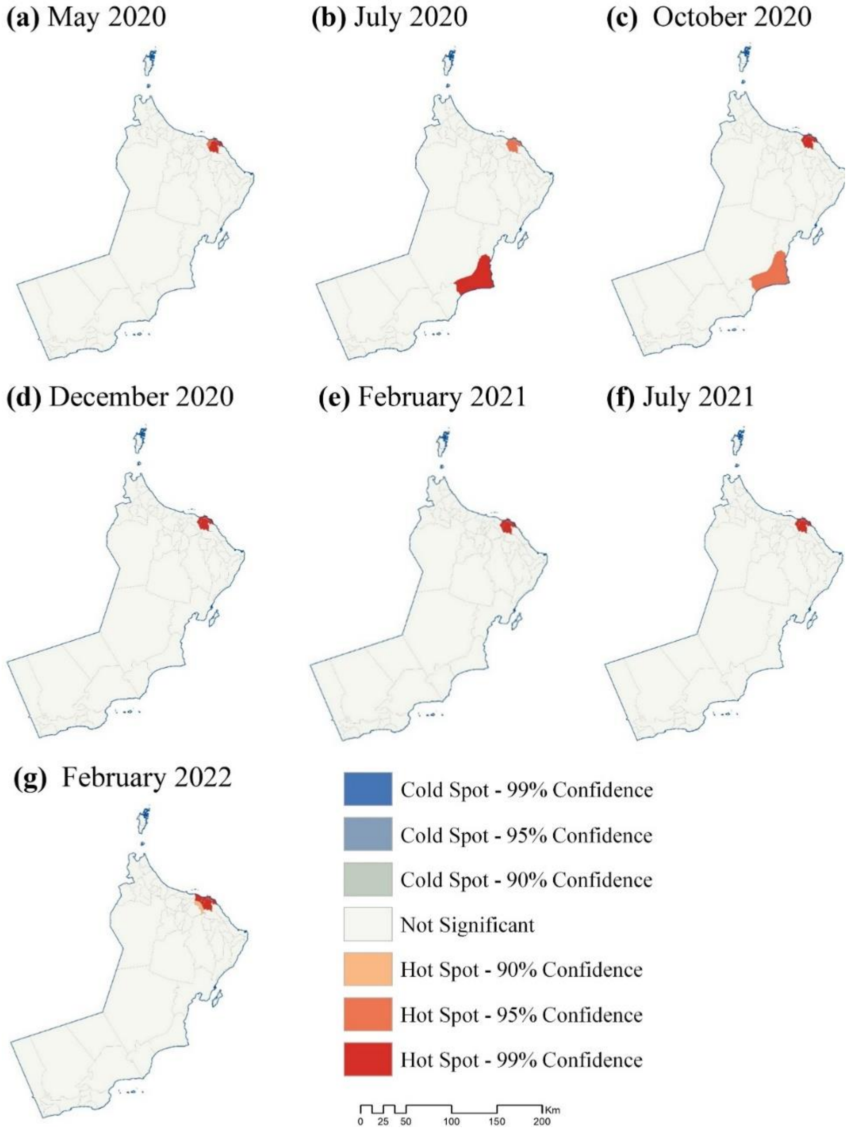


Figure 15. Hotspot output for Oman during the study period; (a) from May to July 2020, (b) from July to October 2020, (c) from October to December 2020, (d) from December 2020 to February 2021, (e) from February to July 2021, (f) from July 2021 to February 2022, (g) during February 2022

## 4. CONCLUSION

Using GIS technology, this study investigated the systematic temporal and geographical distribution of COVID–19 in the Sultanate of Oman throughout a two–year study period. A spatial-temporal analysis of COVID–19 was done using spatial analysis of inverse distance weighted interpolation (IDW) and hotspot analysis for all positive COVID–19 cases to identify the prospective infection areas in the Sultanate of Oman. The analysis revealed that the population distribution and density have a significant correlation with the spatial pattern of the COVID–19 outbreak; the most populated *wilayat* recorded the highest cases of infections.

According to the daily–confirmed cases, we found that the disease has increased by an average of 11.5% on a weekly basis since all *Wilayats* of Muscat Governorate that were locked down in April 2020. However, after the health quarantine was lifted on May 29, 2020, the weekly cases surged in the *Wilayats* of Muscat Governorate to 16.6% of confirmed cases except for Mutrah *Wilayat* where it was still quarantined and the percentage of cases in the *wilayat* decreased from 53.6% by May 14 to 11.1% by July 10, 2020. Al Batinah North and Dhofar Governorates recorded an increase of 32.1% and 30.5% respectively after the restrictions had eased. Consequently, the lockdown was implemented and the percentage of COVID–19 outbreak had decreased to 27.7% in Al Batinah North and 14.6% in Dhofar. In the *Wilayat* of Ad Duqm, the cases of infection explode to 33.0% before it had been isolated from other *wilayat*. Therefore, the spread of COVID–19 dropped off to 1.0% up to the second week of August. However, the spread rose again to 17.5% after lifting the lockdown.

Using hotspot analysis (Getis–Ord GI*), we were able to recognize spatial clusters of high and low intensity of infections. Although the hotspot changed over time, the capital *Wilayats* continuously recorded the highest intensity of infections during the pandemic. It is worthy of note that the guidelines and actions taken by the SC in charge of following up on COVID–19 developments were influenced the daily confirmed cases. This study would be appropriate for pertinent organizations to perform detailed studies for developing the monitoring disease system and dominating relevant factors. Based on the results of this study, the propped methodology can be further applied to any size of population around the globe to study the impact of an epidemic strike. This study suggests using geospatial modeling to manage global epidemics and pandemics by providing valuable insights to support stakeholders with data-driven hot/cold spots analysis for informed decision-making and control strategies.

## REFERENCES


[1] Y. Gao *et al.*, “A cluster of the corona virus disease 2019 caused by incubation period transmission in Wuxi, China,” *Journal of Infection*, vol. 80, no. 6, pp. 666–670, Jun. 2020, doi: 10.1016/j.jinf.2020.03.042.

[2] WHO, “Naming the coronavirus disease (COVID-19) and the virus that causes it,” *World Health Organization*, https://www.who.int/emergencies/diseases/novel-coronavirus-2019/technical-guidance/naming-the-coronavirus-disease-(covid-2019)-and-the-virus-that-causes-it (accessed Aug. 31, 2023).

[3] WHO, “Coronavirus disease 2019 (COVID-19) situation report–51,” *World Health Organization*, 2020. Accessed: Aug. 31, 2023). [Online], Available: https://www.who.int/docs/default-source/coronaviruse/situation-reports/20200311-sitrep-51-covid-19.pdf

[4] J. K. Wardman and R. Lofstedt, “COVID-19: confronting a new world risk,” *Journal of Risk Research*, vol. 23, no. 7–8, pp. 833–837, Aug. 2020, doi: 10.1080/13669877.2020.1842988.

[5] I. Franch-Pardo, M. R. Desjardins, I. Barea-Navarro, and A. Cerdà, “A review of GIS methodologies to analyze the dynamics of COVID-19 in the second half of 2020,” *Transactions in GIS*, vol. 25, no. 5, pp. 2191–2239, Oct. 2021, doi: 10.1111/tgis.12792.

[6] M. Abed Alah, S. Abdeen, and V. Kehyayan, “The first few cases and fatalities of corona virus disease 2019 (COVID-19) in the Eastern Mediterranean Region of the World Health Organization: a rapid review,” *Journal of Infection and Public Health*, vol. 13, no. 10, pp. 1367–1372, Oct. 2020, doi: 10.1016/j.jiph.2020.06.009.

[7] Ministry of Health, “Statements No. 1-43,” *Ministry of Health Sultanate of Oman*, https://www.moh.gov.om/en/-59 (accessed Aug. 31, 2023).

[8] T. Al Ghafri *et al.*, “Responses to the pandemic COVID-19 in Primary Health Care in Oman: Muscat Experience,” *Oman Medical Journal*, vol. 36, no. 1, pp. e216--e216, Jan. 2021, doi: 10.5001/omj.2020.70.

[9] Oman Government Communication, “OmanVSCovid19,” *x.com*, https://x.com/OmanVSCovid19 (accessed Aug. 31, 2023).

[10] WHO, “Coronavirus disease 2019 (COVID-19) situation report 51,” *Situation Report, World Health Organization*, 2020. https://www.un.org/unispal/document/coronavirus-disease-2019-covid-19-situation-report-51/ (accessed Aug. 31, 2023).

[11] K. Azuma, U. Yanagi, N. Kagi, H. Kim, M. Ogata, and M. Hayashi, “Environmental factors involved in SARS-CoV-2 transmission: effect and role of indoor environmental quality in the strategy for COVID-19 infection control,” *Environmental Health and Preventive Medicine*, vol. 25, no. 1, Dec. 2020, doi: 10.1186/s12199-020-00904-2.

[12] H.-Y. Cheng, S.-W. Jian, D.-P. Liu, T.-C. Ng, W.-T. Huang, and H.-H. Lin, “Contact tracing assessment of COVID-19 transmission dynamics in Taiwan and risk at different exposure periods before and after symptom onset,” *JAMA Internal Medicine*, vol. 180, no. 9, Sep. 2020, doi: 10.1001/jamainternmed.2020.2020.

[13] L. A. Waller and C. A. Gotway, *Applied spatial statistics for public health data*. Wiley, 2004.

[14] L. Gosoniu, A. Msengwa, C. Lengeler, and P. Vounatsou, “Spatially explicit burden estimates of malaria in Tanzania: Bayesian geostatistical modeling of the malaria indicator survey data,” *PLoS ONE*, vol. 7, no. 5, May 2012, doi: 10.1371/journal.pone.0023966.

[15] Z. Ren *et al.*, “Predicting malaria vector distribution under climate change scenarios in China: challenges for malaria elimination,” *Scientific Reports*, vol. 6, no. 1, Feb. 2016, doi: 10.1038/srep20604.

[16] M. Mathur, “Spatial autocorrelation analysis in plant population: an overview,” *Journal of Applied and Natural Science*, vol. 7, no. 1, pp. 501–513, Jun. 2015, doi: 10.31018/jans.v7i1.639.

[17] L. I. Zambrano *et al.*, “Estimating and mapping the incidence of dengue and chikungunya in Honduras during 2015 using Geographic Information Systems (GIS),” *Journal of Infection and Public Health*, vol. 10, no. 4, pp. 446–456, Jul. 2017, doi: 10.1016/j.jiph.2016.08.003.

[18] S. Sarwar, R. Waheed, S. Sarwar, and A. Khan, “COVID-19 challenges to Pakistan: Is GIS analysis useful to draw solutions?,” *Science of The Total Environment*, vol. 730, Aug. 2020, doi: 10.1016/j.scitotenv.2020.139089.

[19] M. S. Haider, S. K. Salih, S. Hassan, N. J. Taniwall, M. F. U. Moazzam, and B. G. Lee, “Spatial distribution and mapping of COVID-19 pandemic in Afghanistan using GIS technique,” *SN Social Sciences*, vol. 2, no. 5, May 2022, doi: 10.1007/s43545-

022-00349-0.
[20] National Center for Statistics and Information, "Results of electronic census 2020," *ecensus.gov.om*, 2021. https://ecensus.gov.om/ecen-portal/?lang=en (accessed Aug. 31, 2023).
[21] F. Parvin, S. A. Ali, S. N. I. Hashmi, and A. Ahmad, "Spatial prediction and mapping of the COVID-19 hotspot in India using geostatistical technique," *Spatial Information Research*, vol. 29, no. 4, pp. 479–494, Aug. 2021, doi: 10.1007/s41324-020-00375-1.
[22] A. Islam, M. A. Sayeed, M. K. Rahman, J. Ferdous, S. Islam, and M. M. Hassan, "Geospatial dynamics of COVID-19 clusters and hotspots in Bangladesh," *Transboundary and Emerging Diseases*, vol. 68, no. 6, pp. 3643–3657, Nov. 2021, doi: 10.1111/tbed.13973.
[23] M. Shariati, T. Mesgari, M. Kasraee, and M. Jahangiri-rad, "Spatiotemporal analysis and hotspots detection of COVID-19 using geographic information system (March and April, 2020)," *Journal of Environmental Health Science and Engineering*, vol. 18, no. 2, pp. 1499–1507, Dec. 2020, doi: 10.1007/s40201-020-00565-x.
[24] M. Fatima, S. Arshad, I. Butt, and S. Arshad, "Geospatial clustering and hot spot detection of COVID-19 incidence in 2020: a global analysis," *International Journal of Geospatial and Environmental Research*, vol. 8, no. 1, 2021.
[25] N. Kianfar and M. S. Mesgari, "GIS-based spatio-temporal analysis and modeling of COVID-19 incidence rates in Europe," *Spatial and Spatio-temporal Epidemiology*, vol. 41, Jun. 2022, doi: 10.1016/j.sste.2022.100498.
[26] K. M. Al-Kindi *et al.*, "Spatiotemporal assessment of COVID-19 spread over Oman using GIS techniques," *Earth Systems and Environment*, vol. 4, no. 4, pp. 797–811, Dec. 2020, doi: 10.1007/s41748-020-00194-2.
[27] K. M. Al Kindi *et al.*, "Demographic and socioeconomic determinants of COVID-19 across Oman - a geospatial modelling approach," *Geospatial Health*, vol. 16, no. 1, May 2021, doi: 10.4081/gh.2021.985.
[28] S. Mansour *et al.*, "Spatial associations between COVID-19 incidence rates and work sectors: Geospatial modeling of infection patterns among migrants in Oman," *Annals of the American Association of Geographers*, vol. 112, no. 7, pp. 1974–1993, Oct. 2022, doi: 10.1080/24694452.2021.2015281.
[29] Ministry of information-Sultanate of Oman, "Information portal," *omaninfo.om*, https://omaninfo.om/oman (accessed Dec. 16, 2023).
[30] "Statistical year book 2020," *National Center for Statistics and Information*, 2020. Accessed: Aug. 31, 2023. [Online], Available: https://www.arabdevelopmentportal.com/sites/default/files/publication/bar_statistical_year_book_2020-14_4f5cf07c-02d9-4e13-b7aa-0d6b21912f67.pdf
[31] M. N. Kamel Boulos and E. M. Geraghty, "Geographical tracking and mapping of coronavirus disease COVID-19/severe acute respiratory syndrome coronavirus 2 (SARS-CoV-2) epidemic and associated events around the world: how 21st century GIS technologies are supporting the global fight against outbr," *International Journal of Health Geographics*, vol. 19, no. 1, Dec. 2020, doi: 10.1186/s12942-020-00202-8.
[32] E. Layati, A. Ouigmane, M. de Carvalho Alves, B. Murugesan, and M. El Ghachi, "Spread mapping of Covid-19 in Morocco using Geospatial approach," *Journal of Geographical Studies*, vol. 4, no. 1, pp. 34–43, Sep. 2020, doi: 10.21523/gcj5.20040104.
[33] R. Nasiri *et al.*, "Spatio-temporal analysis of COVID-19 incidence rate using GIS: a case study—Tehran metropolitan, Iran," *GeoJournal*, vol. 87, no. 4, pp. 3291–3305, Aug. 2022, doi: 10.1007/s10708-021-10438-x.
[34] S. Mahmood, "Exploring COVID-19 incidence hotspot in Metropolitan area of Pakistan using geo-statistical approach: a study of Lahore city," *Spatial Information Research*, vol. 30, no. 4, pp. 469–476, Aug. 2022, doi: 10.1007/s41324-021-00423-4.
[35] C. Liu, X. Su, Z. Dong, X. Liu, and C. Qiu, "Understanding COVID-19: comparison of spatio-temporal analysis methods used to study epidemic spread patterns in the United States," *Geospatial Health*, vol. 18, no. 1, May 2023, doi: 10.4081/gh.2023.1200.
[36] N. Nazia, Z. A. Butt, M. L. Bedard, W.-C. Tang, H. Sehar, and J. Law, "Methods used in the spatial and spatiotemporal analysis of COVID-19 epidemiology: a systematic review," *International Journal of Environmental Research and Public Health*, vol. 19, no. 14, Jul. 2022, doi: 10.3390/ijerph19148267.
[37] V. Selvaraj, "Mapping of Covid-19 pandemic in India using interpolation method based on GIS," *Journal of Geography & Natural Disasters*, vol. 11, no. 8, pp. 1–16, 2021.
[38] J. S. Ibarra-Bonilla, F. Villarreal-Guerrero, A. Pinedo-Alvarez, and J. A. Prieto-Amparán, "COVID-19 in Chihuahua, Mexico: Assessing its spatial behaviour through the inverse distance weighted interpolation technique," *Canadian Geographies/ Géographies canadiennes*, vol. 67, no. 4, pp. 470–483, Dec. 2023, doi: 10.1111/cag.12853.
[39] M. F. U. Moazzam, T. U. Paracha, G. Rahman, B. G. Lee, and N. Farid, "Spatial and temporal mapping of COVID-19 pandemic using GIS technique: a case study of Italy," *International Journal of Geoinformatics*, vol. 17, no. 5, pp. 100–108, Oct. 2021, doi: 10.52939/ijg.v17i5.2019.
[40] M. A. Y. Al-Shaheen, A. M. Al-Sayed, and A. Y. Hasan, "GIS-based solutions for monitoring and controlling COVID-19 in ASHGHAL construction projects: improving construction sector resilience," in *Proceedings of the 2nd International Conference on Civil Infrastructure and Construction (CIC 2023)*, Feb. 2023, pp. 234–243, doi: 10.29117/cic.2023.0034.
[41] F. A. Awwad, M. A. Mohamoud, and M. R. Abonazel, "Estimating COVID-19 cases in Makkah region of Saudi Arabia: Space-time ARIMA modeling," *PLOS ONE*, vol. 16, no. 4, p. e0250149, Apr. 2021, doi: 10.1371/journal.pone.0250149.
[42] A. S. Almobarak, H. R. Almohammadi, S. A. Aboalnaser, and L. Syed, "Spatio-temporal analysis of the spread COVID-19 in Saudi Arabia," in *2020 13th International Conference on Developments in eSystems Engineering (DeSE)*, Dec. 2020, pp. 341–346, doi: 10.1109/DeSE51703.2020.9450770.
[43] M. Amamou and K. Ben-Ahmed, "Managing the COVID-19 pandemic in thirty-two policy measures in Saudi Arabia: a mixed-methods analysis," *Journal of Infection and Public Health*, vol. 16, no. 10, pp. 1650–1658, Oct. 2023, doi: 10.1016/j.jiph.2023.08.008.
[44] S. Mansour, A. Al Kindi, A. Al-Said, A. Al-Said, and P. Atkinson, "Sociodemographic determinants of COVID-19 incidence rates in Oman: Geospatial modelling using multiscale geographically weighted regression (MGWR)," *Sustainable Cities and Society*, vol. 65, Feb. 2021, doi: 10.1016/j.scs.2020.102627.
[45] Esri, "How inverse distance weighted interpolation works," *ArcGIS Pro*, https://pro.arcgis.com/en/pro-app/help/analysis/geostatistical-analyst/how-inverse-distance-weighted-interpolation-works.htm (accessed Aug. 31, 2023).
[46] C. Childs, "Interpolating surfaces in ArcGIS spatial analyst," *ArcUser*, vol. 3235, no. 569, pp. 32–35, 2024.
[47] P. M. Bartier and C. P. Keller, "Multivariate interpolation to incorporate thematic surface data using inverse distance weighting (IDW)," *Computers & Geosciences*, vol. 22, no. 7, pp. 795–799, Aug. 1996, doi: 10.1016/0098-3004(96)00021-0.
[48] F. Huang, D. Liu, X. Tan, J. Wang, Y. Chen, and B. He, "Explorations of the implementation of a parallel IDW interpolation algorithm in a Linux cluster-based parallel GIS," *Computers & Geosciences*, vol. 37, no. 4, pp. 426–434, Apr. 2011, doi:

10.1016/j.cageo.2010.05.024.
[49] X. Guan and H. Wu, "Parallel optimization of IDW interpolation algorithm on multicore platform," in *Geoinformatics 2008 and Joint Conference on GIS and Built Environment: Advanced Spatial Data Models and Analyses*, Oct. 2009, p. 71461Y, doi: 10.1117/12.813163.
[50] Esri, "How hot spot analysis (Getis-Ord Gi*) works," *ArcGIS Pro*, https://pro.arcgis.com/en/pro-app/latest/tool-reference/spatial-statistics/h-how-hot-spot-analysis-getis-ord-gi-spatial-stati.htm (accessed Sep. 10, 2023).
[51] Esri, "How spatial autocorrelation (Global Moran's I) works," *ArcGIS Pro*, https://pro.arcgis.com/en/pro-app/latest/tool-reference/spatial-statistics/h-how-spatial-autocorrelation-moran-s-i-spatial-st.htm (accessed Dec. 16, 2023).
[52] S. A. Meo, A. A. Abukhalaf, A. A. Alomar, F. J. AlMutairi, A. M. Usmani, and D. C. Klonoff, "Impact of lockdown on COVID-19 prevalence and mortality during 2020 pandemic: observational analysis of 27 countries," *European Journal of Medical Research*, vol. 25, no. 1, Dec. 2020, doi: 10.1186/s40001-020-00456-9.

## BIOGRAPHIES OF AUTHORS

**Yaseen Al–Mulla** is an associate professor and the director of the remote sensing and GIS Research Center, Sultan Qaboos University, Al-Khod, Sultanate of Oman. He is also Founder and Chair of IEEE GRSS Oman, Scientific Ambassador for IEEE GRSS, an ICESCO chair of remote sensing and machine learning projects, and chair of artificial intelligence in remote sensing and GIS SQU RG. His current research interests include using remote sensing and GIS technologies for environmental assessment/mapping and land use/change. As well as the use of artificial intelligent based sensors, instrumentations, UAV and IoT for real time monitoring/controlling/mapping. He can be contacted at email: yalmula@squ.edu.om.

**Mohammed Al–Muqaimi** is a technician at the Remote Sensing and GIS Research Center, Sultan Qaboos University, Al–Khod, Sultanate of Oman. He holds a B.Sc. in geography from College of Arts, Sultan Qaboos University, Al–Khod, Sultanate of Oman. He has worked with Diwan of Royal Court of Oman as Geospatial analysist, Geodatabase management and other GIS related work. He can be contacted at: m.almuqaimi@squ.edu.om.

**Ahsan Ali** is a postdoctoral researcher at the remote sensing and GIS Research Center, Sultan Qaboos University, Al–Khod, Sultanate of Oman. He has received his B.Sc. in agriculture engineering and M.Sc. in water resources management from University of Agriculture, Faisalabad, Pakistan. He also received a Ph.D. degree in soil and water management from college of Agricultural and Marine Sciences, Sultan Qaboos University, Oman. His research interest included the application of remote sensing and GIS, deep learning and AI application in the agriculture, soil and water monitoring. He can be contacted at emails: a.ali@squ.edu.om.

**Taif Al–Badi** is a research assistant at the Remote Sensing and GIS Research Center, Sultan Qaboos University, Al–Khod, Sultanate of Oman. She holds a B.Sc. in electrical and computer engineer, Sultan Qaboos University, Al–Khod, Sultanate of Oman. She served as a president of IEEE SQU Society between 2019 and 2020. She has very good skills in programming languages and simulation programs, such as C++/C, python, Arduino IDE, Android Studio, HTML, CSS, PHP, SQL, PSpice, LabView, MATLAB, and Protus. She can be contacted at: taifalbadi123@gmail.com.

**Krishna Parimi** is a research assistant at the Remote Sensing and GIS Research Center, Sultan Qaboos University, Al–Khod, Sultanate of Oman. He has received his B.Tech. in geo informatics from University of Petroleum and Energy Studies, India, and his M.Tech. in geographic information systems from NIIT University, India. His research interest included the application of geographic information systems, remote sensing, spatio temporal analysis, as well as object-based identification using deep learning techniques. He can be contacted at emails: krishna.nihar7@gmail.com.

**Anusha Chowdary** is a research assistant at the Remote Sensing and GIS Research Center, Sultan Qaboos University, Al–Khod, Sultanate of Oman. Ms. Choudhry worked on the mapping aspect of the gathered covid data using advanced tools of the ArcGIS online platform. She can be contacted at emails: anushadevi3959@gmail.com.